CONSISTENT TRANSPORT COEFFICIENTS IN ASTROPHYSICS

JUAN M. FONTENLA*#
Space Science Laboratory,
NASA Marshall Space Flight Center
Huntsville, AL

M. ROVIRA#
Instituto de Astronomia y Fisica del Espacio, CONICET

C. FERRO FONTAN#
Facultad de Ciencias Exactas Y Naturales, UBA

(NASA-TM-101154) CONSISTENT TRANSPORT COEFFICIENTS IN ASTROPHYSICS (NASA) 75 p
CSCL 03B

N88-24560

Unclas
G3/90 0146682

*NAS/NRC Research Associate.
#Member of the Carrera del Investigador, CONICET, Argentina.

ABSTRACT

We develop a consistent theory for dealing with transport phenomena in stellar atmospheres starting with the kinetic equations and introducing the three cases: LTE, partial LTE (usually called non-LTE), and non-LTE (nonlocal distribution functions). We present the consistent hydrodynamical equations for partial-LTE, define transport coefficients, and show a method to calculate them. The method is based on the numerical solution of kinetic equations considering Landau, Boltzmann, and Focker-Planck collision terms. Finally we show a set of results for the transport coefficients derived for a partially ionized hydrogen gas with radiation, considering ionization and recombination as well as elastic collisions. The results obtained imply major changes in some types of theoretical model calculations and can resolve some important current problems concerning energy and mass balance in the solar atmosphere. We show that energy balance in the lower solar transition region can be fully explained by means of radiation losses and conductive flux.

I. INTRODUCTION

We do not need to document the enormous importance that transport phenomena have in stellar atmospheres, as well as in most areas of physics; we only mention here that thermal conduction is the key to understanding the solar transition region and that ambipolar diffusion can be very important for the mass and energy transport perpendicular to the magnetic field.

By transport phenomena we mean the macroscopic transport associated with matter, excluding radiation. Radiation processes have been thoroughly treated since the beginning of astrophysical research. See Athay (1972) and Mihalas (1978).

Standard transport theories have been developed in the context of laboratory physics for cases where radiation is negligible and LTE prevails (implying small gradients of physical parameters as well as a small radiation flux). In that context, the early work by Chapman, Enskog, and Brunet (hereafter CHEB), as discussed by Chapman and Cowling (1936, hereafter CC), led to a complete compilation of transport coefficients, definitions, and calculation methods for non-ionized gases; the work by Braginskii (1965) gives the results of applying CHEB methods to highly ionized gases (plasmas) and some additional definitions of frictional coefficients very usefull in laboratory experiments. Hochestim (1967) has made more accurate derivations of transport coefficients using that method.

The case of a partially ionized hydrogen gas has been treated by Devoto (1966, 1968) based on CHEB methods, but these results again refer to laboratory conditions (particularly high

pressure around 1 atm). Following the same formalism, Nowak and Ulmschneider (1977) have calculated the thermal conductivities for pressure values covering the range of interest in astrophysics. These last three papers consider neither radiation nor inelastic collisions.

We mention also the different approach followed by Spitzer and Harm (1953) where not only the transport coefficients but also the first order distribution function was numerically calculated for a fully ionized gas without restriction to a truncated polynomial expansion.

The results of Spitzer and Harm (hereafter SH) have been used extensively in several fields of physics and also show the limits of validity of the transport coefficients. The SH results let to the analytical approach of Shvarts et al. (1981) for calculating flux limit coefficients which have been qualitatively confirmed by experiments. An analytical approach applied by Campbell (1984) also shows a detailed calculation of the first order distribution function for very simplified cases.

Here, we stress that these approaches imply the direct solution of a set of kinetic equations for a fully ionized gas, which are expressed with Focker-Planck collision terms, instead of the Boltzmann term as in the CHEB method.

An approach that fits the capabilities of modern "supercomputers" has been suggested by Fontenla (1985) showing how one can define a set of transport coefficients and calculate them by numerical methods for cases of astrophysical interest where LTE cannot be assumed. This approach also deals with

partial-LTE (p-LTE) conditions and suggests a method for cases where even p-LTE does not apply. A similar numerical method has been used by Epperlein and Haines (1986) for a fully ionized gas with a magnetic field, but again without considering radiation and inelastic collisions. Another related paper by Luciani, Mora, and Pellat (1985) assumes a simplified kinetic equation and calculates an approach to the non-localized conductive flux that arises when p-LTE starts to fail (this is done for a fully ionized gas without inelastic collisions). Calculations of non-local effects also have been carried out by Shoub (1983), and by Owocki and Canfield (1986) for the solar transition region.

In the present paper we show a set of hydrodynamical equations derived from the kinetic equations which applies to stellar atmospheres without any apriori assumptions regarding the distribution functions or the radiation field. Thus, for plane parallel cases we show one can develop the kinetic equations (and radiative transfer equations) in a formulation with symmetrical and antisymmetrical parts, that characterizes 1) the LTE regime as having the particle and photon distribution functions close to Maxwell's and Planck's formulae, 2) p-LTE when only the first holds, and 3) non-LTE when neither applies. Then, we apply the method by Fontenla (1985) to compute a consistent set of transfer coefficients in the p-LTE, plane-parallel case, for a partially ionized hydrogen gas with a radiation field.

II. THE HYDRODYNAMICAL EQUATIONS

These equations can be derived from the moments of the kinetic equations considering only particles (i.e., excluding radiation), and differs from some others which include radiation in the moments of the kinetic equations (see for example Anderson, 1976). The reason for the present formulation lies in the fact that for most cases in stellar atmospheres the radiation spectrum has to be solved in detail, and its agreement with observations is the main goal.

Since the inelastic collision terms do not vanish when taking the moments of the kinetic equations, one is left with the moments of the Boltzmann collision term ξ_α for the α particles

$$R_\alpha = \int \xi_\alpha d\pi_\alpha ; \quad \vec{P}_\alpha = \int m_\alpha \vec{v} \xi_\alpha d\pi_\alpha ; \quad \varepsilon_\alpha = \int m_\alpha \frac{v^2}{2} \xi_\alpha d\pi_\alpha ,$$

where $d\pi_\alpha$ is the impulse phase-space volume element and m_α is the mass of particles of species α.

With those definitions, the statistical equilibrium equations result in

$$\frac{\partial n_\alpha}{\partial t} + \nabla\cdot(n_\alpha \vec{V}_\alpha) + \nabla\cdot(n_\alpha \vec{U}) = R_\alpha ,$$

where n_α is the number density of α particles, $\vec{V}_\alpha$ is the diffusion velocity, $\vec{U}$ is the fluid velocity (mass center velocity), and R_α is the net rate of creation of α particles per volume unit.

Since mass is conserved in collisions, the usual mass conservation equation holds

$$\frac{\partial \rho}{\partial t} + \nabla \cdot (\rho \vec{U}) = 0,$$

where ρ is the mass density.

Taking the first momemt of the kinetic equations we find

$$\frac{\partial (\rho \vec{U})}{\partial t} + \nabla \cdot (\overline{\overline{\pi}}) = \vec{F} + \vec{P}$$

where

$$F = \sum_{\alpha} \rho_{\alpha} \vec{g}_{\alpha} , \quad \vec{P} = \sum_{\alpha} \vec{P}_{\alpha} , \quad \rho_{\alpha} = n_{\alpha} m_{\alpha}$$

and $\vec{g}_{\alpha}$ is the acceleration experinced by an α particle due to external (or autoconsistent) fields. Then the definition of the force $\vec{F}$ per volume unit experienced by the whole gas of matter and $\vec{P}$, results the net gain of particle impulse per volume unit due to the inelastic collisions. The last quantity equals the net loss of photon impulse and can be expressed in terms of the collisional term for radiation

$$\vec{P} = \frac{1}{c} \int (\kappa_{\nu} I_{\nu} - \varepsilon_{\nu}) \vec{n} \, d\omega \, d\nu,$$

where c is the speed of light, κ_{ν}, I_{ν}, and ε_{ν} have their usual meaning of absorption coefficient, intensity and emissivity of radiation at frequency ν and with direction $\vec{n}$, and $d\omega$ is the solid angle element.

The tensor $\bar{\bar{\pi}}$ contains the pressure p, the viscous stress $\bar{\bar{\Gamma}}$ (of null trace), and the terms due to diffusion

$$\bar{\bar{\pi}} = p\,\bar{\bar{I}} + \bar{\bar{\Gamma}} + \sum_\alpha \rho_\alpha \vec{V}_\alpha \vec{V}_\alpha$$

where

$$p = \sum_\alpha p_\alpha,\quad p_\alpha = \frac{1}{3}\,Tr \int m_\alpha \vec{w}\,\vec{w}\, f_\alpha d\pi_\alpha$$

and the definition $\vec{w} = \vec{v} - (\vec{U} + \vec{V}_\alpha)$. In these equations one usually drops the last term because it is quadratic in V_α.

For stellar atmospheres , when the photon flight time over a characteristic length is small, from the expression of the kinetic equation for photons results

$$\vec{P} = \frac{1}{c}\,\nabla \cdot \int \vec{n}\,\vec{n}\, I_\nu\, d\omega\, d\nu.$$

The kinetic energy equation for the matter gas is

$$\frac{\partial}{\partial t}\left(\frac{3}{2}\,p + \sum_\alpha \rho_\alpha \frac{V_\alpha^2}{2}\right) + \nabla \cdot \left[\vec{U}\left(\frac{3}{2}\,p + \sum_\alpha \rho_\alpha \frac{V_\alpha^2}{2}\right)\right] +$$

$$+ \nabla \cdot \left[\sum_\alpha \vec{V}_\alpha \left(\frac{3}{2}\,p_\alpha + \rho_\alpha \frac{V_\alpha^2}{2}\right)\right] + (\bar{\bar{\pi}} \cdot \nabla) \cdot \vec{U} + \nabla \cdot \left(\sum_\alpha \bar{\bar{\pi}}_\alpha \cdot \vec{V}_\alpha\right) +$$

$$+ \nabla \cdot \vec{q} = \sum_\alpha \rho_\alpha\, \vec{g}_\alpha \cdot \vec{V}_\alpha + \varepsilon - \vec{U} \cdot \vec{P},$$

with $\varepsilon = \sum_\alpha \varepsilon_\alpha$ and $\vec{q} = \sum_\alpha \vec{q}_\alpha$ and with $\vec{q}_\alpha$ being the conductive energy flux for α particles given by

$$\vec{q}_\alpha = \int \vec{w}\, m_\alpha \frac{w^2}{2} f_\alpha \, d\pi_\alpha .$$

This definition of conductive flux agrees with the one from CC since it does not contain the thermal energy flux due to diffusion

$$\sum_\alpha \left[\vec{V}_\alpha \left(\frac{3}{2} p_\alpha + \rho_\alpha \frac{V_\alpha^2}{2}\right) + \bar{\bar{\pi}}_\alpha \cdot \vec{V}_\alpha\right]$$

or $\sum_\alpha \vec{V}_\alpha \frac{5}{2} p_\alpha$ up to first order in V_α.

The term $\vec{U} \cdot \bar{\bar{P}}$ is frequently dropped for non-relativistic cases. Again, the condition for energy balance in collisions gives

$$\sum_\alpha (\varepsilon_\alpha + R_\alpha E_\alpha) = \int (\kappa_\nu I_\nu - \varepsilon_\nu) \, d\omega \, d\nu ,$$

with E_α being the internal energy per α particle.

There results then

$$\varepsilon = - \sum_\alpha E_\alpha \left[\frac{\partial n_\alpha}{\partial t} + \nabla\cdot(n_\alpha \vec{V}_\alpha) + \nabla\cdot(n_\alpha \vec{U})\right] + \int (\kappa_\nu I_\nu - \varepsilon_\nu) \, d\omega \, d\nu .$$

By using the previous equations one can easily transform the thermal energy equation into the entalpy equation.

III. THE CALCULATION OF TRANSPORT COEFFICIENTS

Here we give an overview of the method used for the calculation of transport coefficients and omit the detailed expressions for many of the symbols used, giving only their definitions.

The basic procedure is the expansion of the kinetic equations for the distribution function f_A of each kind of particle (A means a given species with given impulse coordinates) into two equations, one on the symmetrical f_A^s and the other on the antisymmetrical f_A^a part, with respect to the direction of the physical parameter gradient.

We then write the resultant set of equations in numerical form by assuming a discrete partition in velocity and angle and replace the derivative operators by finite difference expressions and integral operators by sums with appropriate weight factors. The resultant set of algebraic equations can be solved by the multidimensional Newton-Raphson technique, which is equivalent (Fontenla 1985) to the CHEB perturbation scheme for expressing the distribution function.

With the z axis parallel to the physical parameter (ρ,p,T,etc.) gradient and assuming that f_A does not depend on x or y (plane parallel geometry), we can write the kinetic equations

$$\beta\mu \frac{\partial f_A}{\partial z} + \frac{1}{c}\frac{\partial f_A}{\partial t} + (\chi_A + \chi_A')\, f_A + (\Phi_A + \Phi_A')\left(\mu \frac{\partial f_A}{\partial \beta} + \frac{(1-\mu^2)}{\beta}\frac{\partial f_A}{\partial \mu}\right) =$$

$$= \eta_A + \alpha_{A\beta\beta}\frac{\partial^2 f_A}{\partial \beta^2} + \alpha_{A\mu\mu}\frac{\partial^2 f_A}{\partial \mu^2} + \alpha_{A\beta\mu}\frac{\partial^2 f_A}{\partial \beta \partial \mu} + \alpha_{A\beta}\frac{\partial f_A}{\partial \beta} + \alpha_{A\mu}\frac{\partial f_A}{\partial \mu}$$

(1)

with $\beta = v/c$, where v is the velocity and μ the cosine of the angle θ between the impulse and the z axis.

Since in the present formulation we assume all variables are only functions of one spatial coordinate, the only consistent magnetic field would be a homogeneous one with the only nonvanishing component along that coordinate. In such a case, for the low field values (i.e., when the Larmour radius is much larger than the particle free path), the field has no influence on the transport coefficients and was excluded by averaging the kinetic equations over angle ϕ. The coefficients n_A and χ_A are integral functions of the distribution functions of the other kinds of particles and account for the Boltzmann source term and sink coefficient, respectively. Φ_A corresponds to the external (or auto-consistent) force field along the z axis and can be written as

$$\Phi_A = \frac{Z_A e^2}{m_A c^2} E^* + \frac{g}{c^2}$$

with g being the gravitational acceleration, E^* the electric field (divided by e) along the z axis, e the proton electric charge, c the speed of light, Z_A the electric charge (divided by e), and m_A the mass of kind A particles.

The remaining coefficients in equation (1) are related to the Landau or Focker-Planck collision terms in the kinetic equations (Balescu 1975)

$$\chi_A' = \sum_{B,i,j} \int m_A^2 c^2 \frac{\partial G_{ij}}{\partial P_{Ai}} \frac{\partial f_B}{\partial P_{Bj}} d\pi_B \tag{2a}$$

$$\Phi_A' = \sum_{B,j} \int [G_{3j} m_A c \frac{\partial f_B}{\partial P_{Bj}} - m_A c\, f_B \frac{\partial G_{3j}}{\partial P_{Aj}}] d\pi_B$$

and expressions for α_A are deduced from the definition of the operator

$$D_A f_A = \sum_{i,j} \psi_{ij} m_A^2 c^2 \frac{\partial^2 f_A}{\partial P_{Ai} \partial P_{Aj}} = \alpha_{A\beta\beta} \frac{\partial^2 f_A}{\partial \beta^2} + \alpha_{A\mu\mu} \frac{\partial^2 f_A}{\partial \mu^2}$$

$$+ \alpha_{A\beta\mu} \frac{\partial^2 f_A}{\partial \beta \partial \mu} + \alpha_{A\beta} \frac{\partial f_A}{\partial \beta} + \alpha_{A\mu} \frac{\partial f_A}{\partial \mu}, \tag{2b}$$

where

$$\psi_{ij} = \sum_B \int G_{ij} f_B d\pi_B,$$

p_{A_i} is the component of the A particle impulse, and $d\pi_B$ is the space-phase volume element of kind B particles. The customary definition of G_{ij} is

$$G_{ij} = \frac{1}{2m_A^2 c^2} \int \delta P_{Ai} \delta P_{Aj} V_{AB} d\sigma,$$

with δP_{Ai} being the components of the A particle impulse change due to collision with a B particle, V_{AB} the relative velocity, and $d\sigma$ the differential cross section.

We shall not give all the details here, but mention only that the photon scattering (Thompson and Rayleigh) and the elastic collision terms for a heavy species A produced by a much lighter species B are also likely to be treated as Focker-Planck terms giving additional contributions to χ_A', Φ_A' and α_A. This is

the case for the effect on atoms due to collisions with electrons, a situation very difficult to treat using Boltzmann collision terms requiring an extremely fine partition.

Equation (1), with definitions (2), can be expanded in its swmmetrical and antisymmetrical components resulting in an operator formulae

$$O^a f^a + O^s f^s = \eta^s + D^a f^a + D^s f^s$$

and (3)

$$O^s f^a + O^a f^s = \eta^a + D^s f^a + D^a f^s,$$

where the operators O are defined by

$$O^a = \beta\mu \frac{\partial}{\partial z} + (\chi^a + \chi'^a) + (\Phi^s + \Phi'^s)(\mu\frac{\partial}{\partial\beta} + \frac{(1-\mu^2)}{\beta}\frac{\partial}{\partial\mu}) \quad (4)$$

$$O^s = \frac{1}{c}\frac{\partial}{\partial t} + (\chi^s + \chi'^s) + (\Phi^a + \Phi'^a)(\mu\frac{\partial}{\partial\beta} + \frac{(1-\mu^2)}{\beta}\frac{\partial}{\partial\mu}).$$

Expressions (1) - (4) are also valid for photons provided χ'_p, Φ'_p, and α_p are null. Equation (3) for the radiation field is equivalent to the usual Feautrier equations (Mihalas 1978).

Equation (3) can be rewritten numerically by chosing a partition in z, t, v, and μ space, replacing the integrals by sums and derivatives by finite difference quotients. The set of

numerical equations can be solved by applying standard techniques.

Equation (3) covers also stationary or quasi-stationary cases in which the time derivative in (4) can be neglected and the resulting set of equations can be solved by the Newton-Raphson iteration scheme.

In the case of p-LTE radiation, departure from the Planck function (i.e., the equilibrium distribution function) is not negligible, and the particle populations depart from the Boltzmann relation, but the distribution function of particles is close to that of Maxwell's. In this case the convergence of CHEB iteration scheme rules the convergence of the Newton-Raphson method for solving equation (3) for particles, with the radiation distribution function given by the radiative transfer equations.

We want to stress that the p-LTE procedure described below cannot be applied when the particle distribution function departs notably from Maxwellian at some relevant velocities.

When the p-LTE assumption is appropriate, one develops equation (3) up to first order in the distribution functions, resulting in a set of linear equations in f_1^a, f_1^s with independent terms $\beta\mu\frac{\partial F}{\partial z}$, χ_F^a and n_F^a, where F is the zero order distribution function (Maxwell's function) of physical parameters (particle density n_α, temperature T, fluid velocity U, and external force potential (ϕz)), and χ_F^a and n_F^a are the Boltzmann terms due to interaction with photons.

Thus, up to first order, f_1^a is a linear function of physical parameter gradients,the external force Φ and the antisymmetrical part of the radiation intensity (I_ν^a), hereafter called thermodynamic forces.

From the previous hydrodynamical equations and radiative transfer and statistical equilibrium equations, one obtains a complete set of equations for solving the full problem. The moment cut-off procedure is acomplished by the expansion conditions chosen for the distribution function. In these equations one can express the macroscopic fluxes as some transport coefficients multiplied by the thermodynamic forces.

For this p-LTE approach the coefficients have to include fluxes induced by radiation, and the usual transport coefficients depend on the angle-averaged radiation field intensity (mean intensity). In the case where LTE holds, radiation can also be expanded up to first order and a reduced set of transport coefficients can be defined.

One important detail not usually considered (see Mihalas 1984, p. 421) is that if consistency is required, one has to consider, for the absorption and emission coefficients, the values corrected to first order (i.e., accounting for f^a). In this case this results in

$$\mu\frac{\partial f_\nu^{\,a}}{\partial z} + \frac{1}{c}\frac{\partial f_\nu^{\,s}}{\partial t} = \eta_\nu^s - \chi_\nu^a f_\nu^a - \chi_\nu^s f_\nu^{\,s}$$

$$\mu\frac{\partial f_\nu^{\,s}}{\partial z} + \frac{1}{c}\frac{\partial f_\nu^{\,a}}{\partial t} = \eta_\nu^a - \chi_\nu^{\,a} f_\nu^{\,s} - \chi_\nu^{\,s} f_\nu^{\,a} \qquad (5)$$

ν being the frequency and f_ν the distribution function for photons, i.e.,

$$f_\nu = \frac{c^2 I_\nu}{2h\nu^3}.$$

One can then define the optical depth as

$$d\tau = - \chi_\nu^s \, dz = - \kappa_\nu^s \, dz$$

and the symmetrical and antisymmetrical source functions

$$S_\nu^s = \left(\frac{2h\nu^3}{c^2}\right) \frac{\eta_\nu^s}{\chi_\nu^s} = \frac{\varepsilon_\nu^s}{\kappa_\nu^s} \; ; \; S_\nu^a = \left(\frac{2h\nu^3}{c^2}\right) \frac{\eta_\nu^a}{\chi_\nu^s} = \frac{\varepsilon_\nu^a}{\kappa_\nu^s} \, ,$$

as well as the ratio

$$r_\nu^a = \frac{\chi_\nu^a}{\chi_\nu^s} = \frac{\kappa_\nu^a}{\kappa_\nu^s},$$

where S_ν^a and r_ν^a become proportional to the thermodynamic forces.

We then find the following set of equations

$$\mu \frac{\partial I_\nu^a}{\partial \tau} - \frac{1}{\chi_\nu^s c} \frac{\partial I_\nu^s}{\partial t} = I_\nu^s - S_\nu^s + r_\nu^a \, I_\nu^a$$

and (6)

$$\mu \frac{\partial I_\nu^s}{\partial \tau} - \frac{1}{\chi_\nu^s c} \frac{\partial I_\nu^a}{\partial t} = I_\nu^a - S_\nu^a + r_\nu^a \, I_\nu^s.$$

It should be noted that under certain circumstances, terms added to the usual equations can be comparable to say I_ν^a.

One can easily see that the present method can be extended to cases where a non-thermal component of some species is present by treating that component in a similar way as is done for radiation. The only condition required is that its scale of variation must be large compared to the mean-free-path of the bulk of "thermal" particles.

Other effects which may be considered by this method are collective effects such as plasma turbulence. By defining plasmons, solitons, etc., one can set up expressions analogous to kinetic equations and the corresponding interaction terms.

One special point concerning the method we use is the numerical expression adopted for derivatives of f_1^a with respect to v and μ and the considerations which have to be applied to the corresponding limit conditions as well as the integration weight to be used.

For the f_1^a derivatives with respect to μ at intermediate points, we have used the standard finite difference expressions, but for the limit points in our grid, we have assumed

$$f_1^a(\mu) = r\mu + s\mu(1-\mu^2)$$

where r and s were obtained from one limit point to the next.

Regarding the derivatives with respect to v, we have assumed

$$f_1^a(v) = g(v)\ F(v)$$

where F(v) is Maxwell's function and g(v) is a slowly varying function of v, whose derivatives are calculated at intermediate points by the standard finite difference quotients and at the limit points by assuming

$$g = r\, v^n + s\, v^{n+m}.$$

We have taken n = 1 for the first point and n = 3 for the last; m was set equal to 2 for both limits (other values also have been tried with no significant changes noted). The integral weight factors were taken using the same expansion of f_1^a.

The last approach for derivatives and integrals follows from the CHEB method and was also applied by SH. This method allows the use of a coarse partition in v space but it affects the result due to the fact that the adopted form implies certain boundary conditions on the function f_1^a, both at zero and at the high velocity cutoff.

It is beyond the scope of the present paper to discuss the generality of the solutions obtained. We mention only that, as CC stated, accurate results are obtained in the case where the bulk of low-velocity particles are very close to having a Maxwellian distribution, and only the very high energy particles can depart from that distribution.

We have tested the method thoroughly by making detailed comparisons with the f_1^a/F for a fully ionized plasma from our method and the SH results, and for the rigid-sphere gas with the

transport coefficients given by CC. We find remarkable agreement between our computed values and those from SH for low velocities, and we find a substantially lower value for velocities greater than, for instance, twice the thermal velocity. These differences are understandable because SH used a constant Coulomb logarithm and a different cutoff, which does not have any influence on the resulting transport coefficients. The comparison with the rigid-sphere gas gives agreement to within a few tens of percent in the thermal conductivity, which is quite good for our purpose. A comparison also has been made with SH values for the case of a Lorentz gas where there is excellent agreement up to velocities of three or more times the thermal velocity.

IV. THE CALCULATIONS

One of the major goals of the present study is the consideration of both collision terms, the Boltzmann and Fokker-Planck collision terms (the latter in the special form due to Landau, 1936, for charged particles) for neutral particles, charged particles, and photons, considering both elastic and inelastic collisions. This leads us to consider a set of integrodifferential equations for the ensemble of electrons, protons, hydrogen atoms, and photons. In the present approach, we do not account for excited levels of hydrogen atom or other species, and we considered photoionization and radiative recombination as the only inelastic processes (reactive processes

since they change species). At higher temperatures Bremsstrahlung has to be considered, and at high densities collisional ionization and dielectronic recombination must be taken into account.

The effect of Thompson and Rayleigh scattering is small for the range of pressure values considered, and we treat only a two-interval partition in the photon spectrum for low frequencies. However, we have chosen a finely divided partition of frequencies in the range between the head of the Lyman continuum and approximately 285 Å (a frequency 3.2 times that at the head of the Lyman continuum).

In this paper, we have adopted a grid of 20 points in v-space ranging from 0.227 to 5 times the thermal velocity of the species; we have also made calculations changing these values and did not find important differences. Furthermore, the plots shown in Figure 8 demonstrate that the derivatives and integrals of the functions f_1^a vary smoothly between the grid points.

For the angle θ we have considered only three values covering the range from 0° to 90°, and for the ϕ angle we have taken eight values covering the range from 0° to 360°. The steps of the angular partitions are not small, but were taken in order to obtain reasonable computing time and still represent the angular dependence of the first order distribution functions. From the results obtained one sees that the functions f_1^a are nearly linear with μ. This property can be used in further work to simplify the calculations.

In order to get a reasonable set of transport coefficients we have chosen for the medium intensity the formula

$$I_\nu^s = \frac{2h\nu^3}{c^2} \frac{W}{\exp(\frac{h\nu}{kT_R})-1} + F_\nu = \frac{W}{\exp(\frac{h\nu}{kT_R})-1},$$

with h and k being the Planck and Boltzmann constants, respectively, and W and T_R the two free parameters for specifying the intensity and its frequency dependence (see Fontenla and Rovira 1985).

The solution of the transport equations gives

$$I_\nu^a = \mu \frac{\partial I_\nu^s}{\partial \tau} + S_\nu^a - r_\nu^a I_\nu^s \qquad (7)$$

which may be used to relate the values of I_ν^a to the adopted thermodynamic forces Z_W and Z_R, given by

$$Z_W = \frac{d\ln(W)}{dz} \text{ and } Z_R = \frac{d\ln(T_R)}{dz} .$$

In the following we will use (W , T_R) and (Z_W, Z_R) to describe the symmetrical and antisymmetrical parts of the radiation intensity (I_ν^s and I_ν^a respectively).

For the Boltzmann terms we have considered the collision between a pair of incident particles, named A and B, resulting in a pair of emergent paricles, named C and D. The resulting expressions are

$$\chi_A = \int V_{AB} \sigma d\mu_C d\phi_C f_B d\pi_B$$

(8)

$$n_A = \int V_{AB}\ \sigma d\mu_c d\phi_c f_c f_D d\pi_B$$

where $(\sigma d\mu_c d\phi_c)$ is the differential cross section transformed to the fluid rest frame.

The cross section for electron-atom elastic collisions were taken from the computations of Temkin and Lakin (1961), since later publications are in good agreement with these earlier values (Bates 1962; Khan et al. 1982) and show that the errors are small when considering few partial waves.

The atom-atom collisions are far more complicated and calculations have to take into account more than 30 partial waves. However, we are not interested in the fine details of differential cross section which arise from the different wave resonances, but only in the general dependence of cross section with angle and energy. We have used the results of Massey (1971) for the combined cross section

$$d\sigma = \frac{1}{4}\, d\sigma_g + \frac{3}{4}\, d\sigma_u$$

where $d\sigma_g$ and $d\sigma_u$ correspond to the "gerade" and "ungerade" interaction potentials. We notice that the total cross section is almost constant with respect to V_{AB}, except for the sharp resonance at very small velocities. We used a formula giving Massey's value for the total cross section, and the shape of $\sigma(\mu)$ was assumed to be the one corresponding to V_{AB} = 0.6 km s^{-1} (E = 0.004 eV). The shape of σ at higher velocities may be

quite different from the one given by our approach, but there exists no detailed publication in the range of interest. At any rate, since the total cross section is accurate, we do not expect that a change in that shape will produce major errors in our calculations.

In the case of the proton-atom collisions, there is also another physical process, the charge transfer or capture, which is analogous to elastic collision, but seems to be the more important than elastic collision in actual cases (i.e., for small velocities with respect to orbital electron velocity). Again, we have used a formula which gives the total cross section as a function of V_{AB} fitting accurately the experimental data by Fite et al. (1960, 1962) and having reasonable behavior at the low velocity limit according to the theoretical work by Smith (1967). Since we do not have details on the differential cross sections we have assumed that the shape of $\sigma(\mu)$ is given by Opradolce's (1984) expression for the He^+-H charge-exchange collisions.

The cross sections for collisions with photons are taken from Allen (1962) for Thompson and Rayleigh scattering, and for ionization and recombination, assuming dipolar angular properties.

In equation (8) we use for f_c and f_D the velocities v_c and v_D and the angles θ_c and θ_D which are given by the energy and impulse conservation equations. The values of these functions do not correspond to the center of an interval, and for this reason we have scaled those values by assuming $f_1^a = g\ F$ as before. This

procedure minimizes the error, but does not elliminate it. In fact, when considering the Doppler displacement for atom-photon collisions, errors can be important for high velocity atoms.

V. DEFINITION OF TRANSPORT COEFFICIENTS

From our calculations we obtain the coefficients for the functions $f_1^a(v,\mu)$ with respect to gradients in density of all particles (electrons n_e, protons n_p, and atoms n_a), mean particle velocity U (fluid velocity), temperature (T), and radiation parameters (W, T_R), as well as the electric field E*. (We did not calculate variations with respect to gravity g since they are usually negligible in stellar atmospheres.)

By using these values of f_1^a one can calculate the flux of physical quantities such as electric charge (current J), kinetic energy (i.e., thermal flux q_T); one then gets a complete set of transport coefficients. However, the particle densities are not independent. In the first place, charge neutrality ($n_e = n_p$) holds in the cases of interest; otherwise enormous currents arise. Moreover we can assume $\nabla n_e = \nabla n_p$ since the difference would produce strong electric fields which would have an effect larger than the straight gradient difference by a factor $(L/l_D)^2$ (where L is the characteristic length associated with density gradients and l_D is the Debye length); thus, the electric field completely masks the other force.

A set of macroscopic parameters can be chosen such as i, p, U, T, W, T_R, E*, where $i = n_e/n_a$ is the ionization ratio and p is

the gas pressure. In this case it is customary to define the ambipolar diffusion velocity V_A as the mean velocity of atoms with respect to the center of gravity of protons and electrons.

Since we assume ionization is related to the other macroscopic parameters through statistical equilibrium, the degree of ionization is not an independent variable, and

$$Z_i = \frac{n}{2(n_e + n_a)}\left[\frac{3}{2} Z_T - Z_P + Z_W + (1 + X_R)Z_R\right]$$

where

$$Z_i = \frac{d\ln(i)}{dz};\ Z_T = \frac{d\ln(T)}{dz};\ Z_p = \frac{d\ln(P)}{dz}$$

$$Z_W = \frac{d\ln(W)}{dz};\ Z_R = \frac{d\ln(T_R)}{dz};\ Z_U = \frac{1}{c}\frac{dU}{dZ}$$

and where $n = (n_e + n_p + n_a)$, $X_R = h\nu_o/kT_R$, ν_o is the frequency at the head of the Lyman continuum.

This results in a smaller set of independent transport coefficients that relate the fluxes (and, of course, the corrections in the radiative transfer equations, r_ν^a and S_ν^a) to the thermodynamical forces Z_p, Z_U, Z_T, Z_W, Z_R, E^*.

We called these independent transport coefficients Ω_{*p}, Ω_{*U}, Ω_{*T}, Ω_{*W}, etc., where the asterisk has to be replaced by the symbol corresponding to the flux (i.e., A, J, and T for the ambipolar velocity, electric current, and thermal flux, respectively).

It is customary to define the electric conductivity as $\sigma = -\Omega_{JE}$ and to define the coefficients $r_a = -\Omega_{Ja}/\Omega_{JE}$, to give the ratio of the electric field E_a^* which will result in the zero electric current produced by the force Z_a. According to this definition, E_a^* is the value of the electric field which is naturally achieved when the Z_a force is applied and after the electric charge has been redistributed to some equilibrium state, and $r_a = E_a^*/Z_a$.

Customary definitions regarding ambipolar diffusion are confusing and do not apply here because they refer to non reacting species or to cases where the reaction velocity is very small, which is not valid for hydrogen in stellar atmospheres.

We introduce ambipolar diffusion coefficients D_a, which are of importance in astrophysics, by imposing only the condition of null electric current. Then

$$D_a = \Omega_{Aa} + \Omega_{AE}\, r_a .$$

The other transport coefficients of great importance in astrophysics are those related to the thermal conductive flux q, which are customarily defined by subtracting the entalpy flux from the kinetic energy flux q_T. In this case, conditions regarding the anullation of ambipolar velocity are not applicable, and the only consistent restriction is the one regarding electrical equilibrium.

The definition of the thermal conductivity λ leads to the expression

$$\lambda T = \left(\frac{5}{2} kT\ \Omega_{nT} - \Omega_{TT}\right) + r_T\left(\frac{5}{2} kT\ \Omega_{nE} - \Omega_{TE}\right)$$

where Ω_{na} are the coefficients corresponding to the particle flux.

If more species are to be considered, one can define their diffusion velocity with respect to the center of mass, as mentioned above, and all the other coefficient definitions will not be altered since the times involved in reaching the zero diffusion concentration equilibrium are extremely large compared to the characteristic times for other physical processes to occur in stellar atmospheres.

Note that the ambipolar diffusion velocity is not one of the species-diffusion velocities defined previously but forms, with the electric current, a complete and independent set from which the species-diffusion velocities can be derived

$$V_e = - \frac{V_A}{(2 + \gamma)} - \frac{J}{en_e(1 + \gamma)}$$

$$V_p = - \frac{V_A}{(2 + \gamma)} + \frac{J\gamma}{en_e\ (1 + \gamma)}$$

$$V_a = V_A\ \left(\frac{1+\gamma}{2+\gamma}\right)$$

where

$$\gamma = \frac{m_e}{m_p}.$$

When replacing the above formulae in the hydrodynamical equations, the usual Joule heating term appears, as well as the internal energy transport due to ambipolar diffusion.

VI. RESULTS

Using the above definitions, we have calculated the transport coefficients for a grid of physical conditions characterized by the values of p, T, W and T_R (and assuming U = 0). In addition we have also calculated the coefficients for Z_U but since they are of litle interest in most cases, we do not show the results here.

Since all the combinations of values for the physical parameters lead to a large number of possibilities, we have chosen only three sets of values for W and T_R. The first set corresponds to optically thin matter (in the Lyman continuum) lying over the solar chromosphere, such as in solar prominences (W = 0.0022, T_R = 8000 K); the second set accounts for the enhanced radiation field above solar active regions (W = 0.022, T_R = 8000 K); the third set applies to the case of LTE (W = 1, T_R = T).

Table 1 illustrates the grid of values for p and T used in our calculations. In all cases we obtained the ionization from the statistical equilibrium equation neglecting collisional ionization and recombination. We did not include stimulated emission, which is negligible in the cases considered here, since T << 157,600 K.

Neglecting three-body collisions in ionization and recombination is a good aproximation in the present cases (with low pressure values); we have checked the corresponding rates and they are negligible for $p < 1000$ dyne cm^{-2}.

The b_1 value was obtained form the expression

$$b_1 = \frac{E_1(X) - WE_1(X + X_R)}{W\, E_1(X_R)}$$

with $X = h\nu_o/kT$, which for T and T_R <<157,600 K can be approximated by neglecting stimulated emission and by replacing $E_1(x)$ by $x^{-1}\, e^{-x}$. Then

$$b_1 = \frac{T\, e^{X_R}}{WT_R e^{X}} .$$

In the following, values of transport coefficients will be expressed in cgs (ESU) units. We have also defined some standard transport coefficients as reference values. For the electrical conductivity we have chosen Braginskii's (1965) expression for a fully ionized plasma, with $\ln\Lambda = 10$,

$$\sigma_s = 1.4 \times 10^7\, T^{3/2}.$$

For the thermal conductivity we have chosen the SH value given by Allen (1962) (based on $\ln\Lambda = 10$),

$$\lambda_s = 10^{-6}\, T^{5/2}.$$

In the case of the thermoelectric coefficient r_T, we have used the dependence on temperature given by SH,

$$r_{T_s} = 10^3 \, T \, .$$

The standard coefficients given above are provided by a well-established theory for fully ionized hydrogen plasmas. However, the remaining coefficients do not have such standard reference values, so we have chosen these coefficients in order to obtain a smooth variation at the high ionization limit. For the thermo-ambipolar coefficient D_T, we estimate the asymptotic behavior as

$$D_{T_s} = 30 \, T^2 .$$

It is difficult to summarize all the results so we only show the data we believe to be of major importance in stellar atmospheric modeling.

The ratio of the electrical conductivity to its standard value (σ/σ_s) is shown in Figures 1a,b. Note that in Figures 1a and 1b (solar-type and enhanced solar-type radiation fields), the ratio is between 0.4 and 0.8, but in the LTE case shown in Figure 1c, it decreases sharply for $T < 6000$ K (one must remember that for normal astrophysical abundances, because of the contributions of the other elements, the ratio ne/n never drops below 0.0001 which

is the smallest in our calculations). At moderate to high ionization the variation of the ratio with temperature and pressure is due to the variation of the Coulomb logarithm ($\ln \Lambda$). From these results one can estimate the electric conductivity which has to be used when dealing with MHD theory for photospheric or subphotospheric layers of cold stars where magnetic diffusion and Joule heating can be severely underestimated when using Spitzer or Braginskii values.

The thermoelectric coefficient r_T relative to its standard value is plotted in Figures 2. For medium to high ionization, the ratio is almost constant between 0.5 and 0.6. For cases of very small ionization in the LTE case the ratio also goes down very steeply, appearing to have a sharp minimum which is more pronounced for low pressure reaching negative values at some very low ionization, as shown in Figure 2c.

The thermal conductivity (λ) is shown in Figure 3. Note in Fig. 3a that (even at medium ionization) the thermal conductivity can rise to around 40 times the Spitzer value for T = 5000 K, but that it is only slightly higher than the usual value for T = 50,000 K.

Figure 3c shows the asymptotic behavior at low ionization (corresponding to the atom heat flux) and the typical behavior of the fully ionized plasma at the higher ionization. (Again the dependence with temperature and pressure is due to the variation of the Coulomb logarithm.)

Figure 4 shows the shape of the quotient (D_T/D_{T_S}). Parts a and b show that the quotient is almost constant and inversely

proportional to the pressure, except for the case with higher pressure and lower radiation field. However, Fig. 4c shows almost constant values at high ionization that are nearly inversely proportional to pressure, but at low ionization and low pressure, the coefficient reduces and and even changes sign.

Radiation-related coefficients, in turn, are much harder to describe and are not defined by previous theory. Because of the different usage when applying the two types of radiation fields, we have plotted the coefficients regarding the Z_W force for parts a and b and those regarding the Z_R force for parts c of Figures 5, 6, and 7. The standard values were taken as

$$r_{w_s} = -10^5\, T^{1/2};\ r_{R_s} = T^3;$$

$$D_{w_s} = 20\, T^2\ ;\ D_{R_s} = T^3;$$

$$\lambda_{w_s} = T^2\ ;\ \lambda_{R_s} = T^3.$$

From our calculations some numerical noise arises in case of low pressure and high radiation field. This noise can be traced to the fluctuations in the lower density species functions $f_1^a(v)$ and results from the limited numerical quadrature used in the calculations, especially for the photon spectrum and angular variables; usually the fluctuation increases with velocity. One source of this "noise," the Doppler effect on the inelastic collision terms, poses a difficult problem. Here, we simply do not consider the radiative coefficients above the limit where fluctuating values start.

Figure 5a and 5b show the shape of (r_W/r_{W_s}), and Figure 5c shows (r_R/r_{R_s}). The former exhibits an almost constant value for the higher pressure and lower radiation field and a behavior that resembles the D_T curves. Note, however, that the higher pressure and lower radiation intensity is the only case where the r_w coefficient is positive, being lower than zero in the others. Figure 5c shows, however, that for high ionization the ratio is small and inversely proportional to pressure, but is negative and increasing in absolute value as ionization decreases.

Figure 6a and 6b show the values of log (D_W/D_{Ws}), and Fig. 6c shows the value of (D_R/D_{Rs}). Again, Figure 6a and 6b show an almost constant value inversely proportional to the pressure, except for the case of higher pressure and smaller radiation intensity. Figure 6c displays a nearly zero value when temperature increases (in this case it implies both ionization and radiation intensity increases), and negative values nearly inversely proportional to the pressure values when temperature decreases in the grid.

Figure 7a and 7b exhibit the quotient $(\lambda_w/\lambda_{w_s})$, and Figure 7c shows the ratio $(\lambda_R/\lambda_{R_s})$. Note that this coefficient displays higher sensitivity to the inelastic collisions since it gives greater weight to high velocity atoms. It is expected to be the one that reflects the most "noise" in the calculations of the antisymmetrical parts of the atom distribution function.

Figure 7a and 7b show a decreasing ratio with temperature and a slope which increases with decreasing pressure. Figure 7c shows a negative value at low ionization nearly inversely

proportional to pressure, a maximum value,and slowly decreasing values at higher temperatures.

The first-order corrections to the radiative transfer equations can be expressed in terms of the functions f_1^a, since schematically

$$\chi^a = \chi^s \left(\frac{f^a}{f^s}\right)_{\text{atoms}}$$

and

$$S^a = S^s \left[\left(\frac{f^a}{f^s}\right)_{\text{electrons}} + \left(\frac{f^a}{f^s}\right)_{\text{protons}}\right].$$

In these formulas, first-order corrections apply for small values of the thermodynamic forces. In the case of high radiation flux (for instance, in the winds of hot stars), the corrections can rise to zero order, giving very asymmetrical line profiles even in the fluid frame.

Of course, when velocity reaches certain limits depending on thermodynamic force values, the method described gives values of f_1^a which cannot be considered small first-order quantities. At higher velocities and for some angles, our method can give the unphysical result $f_1^a > F$. In such cases, some cutoff procedures are available (Shvarts et al. 1981), which can be introduced in our method. However, if calculations are needed for the realistic distribution function at high velocities, more iterations must be performed on the Newton-Raphson technique, and thus the linear relation between the fluxes and the

thermodynamical forces would not apply. This procedure also fails when locally defined coefficients do not apply, reflecting the departure from p-LTE.

VII. CONCLUSIONS

For the charged particle collision terms, we used only the Landau term in most calculations, but in some of the later computations the Boltzmann term was introduced to account for collisions between charged particles that result in large angles of deflection. From our results, including the Boltzmann term leads to negligible corrections in the principal range of particle velocities.

One limitation of the computational procedure used here is that relativistic corrections were not accounted for in our treatment of particle-photon elastic collisions. Such corrections can affect extreme cases.

From our results, we conclude that it is a fairly good approximation to assume $f_1^a(\mu)$ proportional to μ. However, a polynomial expansion of $f_1^a(v)$ is quite impractical, and we obtain much better numerical behavior by using a finite partition in v-space.

We also conclude that some of the usual theoretical models and the interpretations of observations have to be revised since they have underestimated or neglected important transport phenomena. One of these is the radiation-induced flow in some stellar atmospheres where this flow can play an important role in

the energy balance. Another such case is the solar upper chromosphere and lower transition region where the appropriate values of thermal conductivity can solve some important existing puzzles. For example, we show in Figure 9 the temperature structure of the region according to model C of Vernazza, Avrett, and Loeser (1981). In the region where the steep temperature rise starts, we have plotted the conductive flux corresponding to our ($p = 0.1$ dyne cm^{-2}, $W = 0.0022$, $T_R = 8000$ K) calculated conductivity and the one according to Spitzer's (1962) coefficient. In Fig. 9c we have plotted the conductive flux divergence corresponding to both fluxes. It is striking when comparing this figure with Figure 49 from Vernazza, Avrett, and Loeser that we get flux divergence in this region of the order of the radiative loses, but when using Spitzer's formula, the flux divergence is around an order of magnitude smaller. We believe that proper consideration of transport phenomena can probably explain quite simply the energy balance in this region where all sophisticated energy dissipation explanations have failed (the same can also be true for prominence energy balance; see Fontenla and Rovira 1985).

Another example of the importance of adequate theory for transport phenomena is the energy, impulse, and matter transport across the magnetic fields through atoms (involving ambipolar diffusion), but a consistent theory for this is beyond our paper and would require the consideration of the dependence of the function f_1^a on the angle ϕ (i.e., on the full three dimensions of impulse phase-space).

ACKNOWLEDGEMENTS

We want to thank Drs. E. Tandberg-Hanssen, G. Musielak, and R. Moore for their help in correcting and discussing the manuscript.

REFERENCES

Athay, R.G., 1972, Radiation Transport in Spectral Lines, (Holland: D. Reidel Pub. Co.).

Allen, R., 1962. Astrophysical Quantities (London:Athlone Press).

Anderson, J.L. 1976, Gen. Rel. Grav., 7, 53.

Balescu, R. 1975, Equilibrium and Nonequilibrium Statistical Mechanics (New York: J. Wiley & Sons).

Bates, D.R. 1962, Atomic and Molecular Processes (New York: Academic Press).

Braginskii, S.I. 1965, Reviews of Plasma Physics New York: M. A. Leontovich Consultants Bureau), pp. 205-311.

Campbell, P.M. 1984, Phys. Rev. A., **30**, 365.

Chapman, S., and Cowling, T.G. 1936, The Mathematical Theory of Non Uniform Gases (Cambridge: Cambridge Univ. Press).

Devoto, R.S. 1966, Phys. Fluids, **9**, 1230.

Devoto, R.S. 1968, J. Plasma Phys., **2**, 617.

Epperlein, E.M., and Haines, M.G. 1986, Phys. Fluids, **29**, 1029.

Fite, W.L., Stebbings, R.F., Hummer, D.G., and Brackman, R.T. 1960, Phys. Rev., **119**, 663.

Fite, W.L., Smith, A.C.H., and Stebbings, R.F. 1962, Proc. Royal Soc. A, **268**, 527.

Fontenla, J.M. 1985, Rev. Mexicana Astr. Astrof., **10**, 413.

Fontenla, J.M., and Rovira, M. 1985, Solar Phys., **96**, 53.

Hochestim, A. R. 1967, Proceedings of the Eighth International Conference on Phenomena in Ionized Gases (Vienna: Springer), p. 304.

Khan, P., Dashkan, M., Ghosh, A.S., and Falcon, C. 1982, Phys. Rev. A, **26**, 1401.

Landau, L. 1936, Phys. Z. Sowj. Un., **10**, 154.

Lucinai, J.F., Mora, P., and Pellat, R. 1985, Phys. Fluids, **28**, 835.

Massey, H.S.W. 1971, Electronic and Ionic Impact Phenomena, vol. III (Oxford: Clarendon Press).

Mihalas, D. 1978, Stellar Atmospheres (San Francisco: Freeman).

Mihalas, D., and Weibel Mihalas, B. 1984, Foundations of Radiation Hydrodynamics (New York: Oxford Univ. Press).

Nowak, T., and Ulmschneider P. 1977, Astron. Astrophys., **60**, 413.

Opradolce, L. 1984, private communication.

Owocki, S. P. and Canfield, R. C. 1986, Ap. J., **300**, 265.

Shoub, E. C. 1983, Ap. J., **266**, 339.

Shvarts, D., Delecttrez, J., Mac Crory, R.L., and Verdon, C.P. 1981, Phys. Rev. Letters, **47**, 247.

Smith, F.J. 1967, Proc. Phys. Soc., **92**, 866.

Spitzer, L., and Harm, R. 1953, Phys. Rev., **89**, 977.

Spitzer, L., 1962, Physics of Ionized Gases (New York: Interscience).

Temkin, A., and Lakin, J.C. 1961, Phys. Rev., **121**, 788.

Vernazza, J.E., Avrett, E.H., and Loeser, R. 1981, Ap. J. Supp. Series, **45**, 635.

FIGURE CAPTIONS

FIG. 1a. - Log (σ/σ_s) for solar-type radiation field (W=0.0022, T_R=8000 K) for log p = 0, -1,-2.

FIG. 1b. - Log (σ/σ_s) for enhanced solar-type radiation field (W=0.022, T_R=8000 K) and log p = 0, -1, -2. The curve labeled s corresponds to W=0.1, T_R=8000 K, and log p = 1.

FIG. 1c. - Log (σ/σ_s) for LTE-type radiation field (W=1, T_R=T) and log p = 0, 1, 2, 3.

FIG. 2. - Same as Fig. 1 except for the ratio (r_T/r_{T_s}).

FIG. 3. - Same as Fig. 1 except for the ratio (λ/λ_s).

FIG. 4. - Same as Fig. 1 except for the ratio (D_T/D_{T_s}).

FIG. 5. - Ratio (r_w/r_{w_s}) for solar-type radiation field (W=0.0022, T_R=8000 K) (part a), for enhanced solar-type radiation field (W=0.022 , T_R=8000 K) (part b). Labeled s curve corresponds to p=10 dyne cm^{-2}, W=0.1,T_R=8000 K. Ratio (r_R/r_{R_s}) for LTE-type radiation field (W=1, T_R=T) (part c). Curve label identifying the logarithm of pressure.

FIG. 6. - Same as Fig. 5 except for the ratios (D_W/D_{W_s}) and (D_R/D_{R_s}).

FIG. 7. - Same as Fig. 5 except for the ratios (λ_W/λ_{W_s}) and (λ_R/λ_{R_s}).

FIG. 8. - Quotient ($f_1^a/\mu F Z_a$), for electrons for cases with p=10 dyne cm^{-2} and T=5000 K, W=1, T_R=T (a); T=10,000 K, W=1, T_R=T (b); T=50,000 K, W=1, T_R=T (c); and T=50,000, W=0.1, T_R=8000 K (d).

FIG. 9. - Conductive heat flux in Vernazza, Avrett, and Loeser, Model C. Part a shows, for a part of that model, the temperature T (in K) as a function of the logarithm of mass column (in g cm^{-2}). Part b shows the run of the logarithm of the heat flux (in erg cm^{-2} s^{-1}) for the usual SH formula and from the actual calculations (with solar-type radiation field and pressure p=0.1 dyne cm^{-2}). In part c the logarithm of the flux divergence is plotted from the shown conductive fluxes.

JUAN M. FONTENLA: ES52/Marshall Space Flight
Huntsville, AL 35812, U.S.A.

MARTA ROVIRA: Instituto de Astronomia y Fisica del Espacio
C.C. 67 Suc. 28
1428 Capital, Argentina

CONSTANTINO FERRO FONTAN: Instituto de Astronomia y Fisica del Espacio
C.C. 67 Suc. 28
1428 Capital, Argentina

TABLE 1
Parameters Used in Calculations

Case	p	W	T
1SC	1E-2	2.2E-3	8E3
2SC	1E-1	2.2E-3	8E3
3SC	1E0	2.2E-3	8E3
1SE	1E-2	2.2E-2	8E3
2SE	1E-1	2.2E-2	8E3
3SE	1E0	2.2E-2	8E3
4FM	1E1	1.0E-1	8E3
3ET	1E0	1.0E+0	T
4ET	1E1	1.0E+0	T
5ET	1E2	1.0E+0	T
6ET	1E3	1.0E+0	T

APPENDIX
TABLES OF COEFFICIENTS

TABLE 2
Electrical Conductivity

T	1SC	2SC	3SC	1SE	2SE	3SE	4FM	3ET	4ET	5ET	6ET
5.00E+03	3.33E+12	3.56E+12	3.71E+12	3.37E+12	3.71E+12	4.00E+12	4.45E+12	1.96E+12	1.10E+12	4.71E+11	1.75E+11
6.00E+03	4.24E+12	4.54E+12	4.72E+12	4.29E+12	4.72E+12	5.09E+12	5.63E+12	4.51E+12	4.26E+12	3.29E+12	1.87E+12
8.00E+03	6.24E+12	6.67E+12	6.90E+12	6.29E+12	6.90E+12	7.43E+12	8.19E+12	7.77E+12	8.66E+12	9.36E+12	9.41E+12
1.00E+04	8.42E+12	9.01E+12	9.28E+12	8.47E+12	9.28E+12	9.99E+12	1.10E+13	1.04E+13	1.17E+13	1.34E+13	1.53E+13
1.50E+04	1.46E+13	1.56E+13	1.60E+13	1.46E+13	1.59E+13	1.72E+13	1.87E+13	1.77E+13	1.98E+13	2.24E+13	2.59E+13
2.00E+04	2.15E+13	2.30E+13	2.36E+13	2.16E+13	2.35E+13	2.52E+13	2.75E+13	2.59E+13	2.88E+13	3.24E+13	3.70E+13
2.50E+04	2.91E+13	3.12E+13	3.19E+13	2.92E+13	3.17E+13	3.41E+13	3.70E+13	3.48E+13	3.85E+13	4.32E+13	4.90E+13
3.00E+04	3.73E+13	4.00E+13	4.10E+13	3.74E+13	4.05E+13	4.36E+13	4.73E+13	4.44E+13	4.90E+13	5.47E+13	6.18E+13
4.00E+04	5.53E+13	5.92E+13	6.10E+13	5.54E+13	5.99E+13	6.45E+13	6.98E+13	6.53E+13	7.18E+13	7.96E+13	8.93E+13
5.00E+04	7.52E+13	8.04E+13	8.32E+13	7.52E+13	8.11E+13	8.73E+13	9.45E+13	8.83E+13	9.66E+13	1.07E+14	1.19E+14

TABLE 3
Thermoelectric Coefficient

T	1SC	2SC	3SC	1SE	2SE	3SE	4FM	3ET	4ET	5ET	6ET
5.00E+03	3.11E+06	4.39E+06	1.97E+07	2.76E+06	3.12E+06	4.40E+06	5.53E+06	6.67E+05	4.81E+05	-5.83E+04	-4.32E+05
6.00E+03	3.64E+06	4.99E+06	1.72E+07	3.29E+06	3.65E+06	5.00E+06	6.13E+06	-4.52E+07	-5.74E+05	1.06E+06	8.79E+05
8.00E+03	4.70E+06	6.18E+06	1.61E+07	4.36E+06	4.71E+06	6.19E+06	7.36E+06	4.44E+06	5.05E+06	7.37E+06	3.25E+06
1.00E+04	5.75E+06	7.34E+06	1.63E+07	5.43E+06	5.77E+06	7.35E+06	8.57E+06	5.42E+06	5.46E+06	5.60E+06	6.44E+06
1.50E+04	8.39E+06	1.01E+07	1.85E+07	8.11E+06	8.41E+06	1.01E+07	1.15E+07	8.11E+06	8.14E+06	8.17E+06	8.22E+06
2.00E+04	1.10E+07	1.28E+07	2.12E+07	1.08E+07	1.11E+07	1.29E+07	1.44E+07	1.08E+07	1.08E+07	1.09E+07	1.09E+07
2.50E+04	1.37E+07	1.55E+07	2.41E+07	1.35E+07	1.37E+07	1.55E+07	1.71E+07	1.35E+07	1.35E+07	1.36E+07	1.36E+07
3.00E+04	1.64E+07	1.82E+07	2.69E+07	1.61E+07	1.64E+07	1.82E+07	1.99E+07	1.62E+07	1.62E+07	1.63E+07	1.63E+07
4.00E+04	2.17E+07	2.34E+07	3.26E+07	2.15E+07	2.17E+07	2.35E+07	2.53E+07	2.15E+07	2.16E+07	2.17E+07	2.17E+07
5.00E+04	2.70E+07	2.87E+07	3.82E+07	2.68E+07	2.71E+07	2.87E+07	3.06E+07	2.69E+07	2.70E+07	2.70E+07	2.71E+07

TABLE 4
Thermal Conductivity

T	1SC	2SC	3SC	1SE	2SE	3SE	4FM	3ET	4ET	5ET	6ET
5.00E+03	3.30E+04	6.18E+04	1.14E+05	9.59E+03	3.33E+04	6.22E+04	7.19E+04	7.39E+04	7.31E+04	7.24E+04	7.21E+04
6.00E+03	3.46E+04	6.72E+04	1.13E+05	1.05E+04	3.51E+04	6.77E+04	7.84E+04	6.84E+04	8.14E+04	8.28E+04	8.12E+04
8.00E+03	3.86E+04	7.80E+04	1.21E+05	1.38E+04	3.94E+04	7.90E+04	9.19E+04	2.10E+04	5.54E+04	9.35E+04	8.72E+04
1.00E+04	4.38E+04	8.95E+04	1.34E+05	1.90E+04	4.52E+04	9.12E+04	1.06E+05	1.74E+04	2.12E+04	3.62E+04	7.94E+04
1.50E+04	6.46E+04	1.24E+05	1.76E+05	4.05E+04	6.80E+04	1.28E+05	1.50E+05	4.41E+04	4.92E+04	5.56E+04	6.43E+04
2.00E+04	9.84E+04	1.69E+05	2.31E+05	7.55E+04	1.05E+05	1.77E+05	2.07E+05	8.61E+04	9.55E+04	1.07E+05	1.22E+05
2.50E+04	1.47E+05	2.29E+05	3.02E+05	1.25E+05	1.57E+05	2.41E+05	2.81E+05	1.45E+05	1.60E+05	1.79E+05	2.02E+05
3.00E+04	2.11E+05	3.04E+05	3.89E+05	1.91E+05	2.27E+05	3.22E+05	3.73E+05	2.22E+05	2.44E+05	2.72E+05	3.06E+05
4.00E+04	3.93E+05	5.06E+05	6.20E+05	3.74E+05	4.23E+05	5.41E+05	6.18E+05	4.36E+05	4.78E+05	5.28E+05	5.91E+05
5.00E+04	6.50E+05	7.87E+05	9.34E+05	6.32E+05	6.99E+05	8.44E+05	9.53E+05	7.37E+05	8.05E+05	8.87E+05	9.87E+05

TABLE 5
Thermoambipolar Coefficient

T	1SC	2SC	3SC	1SE	2SE	3SE	4FM	3ET	4ET	5ET	6ET
5.00E+03	9.44E+10	1.46E+10	9.55E+09	8.93E+10	9.44E+09	1.46E+09	2.04E+08	-5.75E+08	-2.83E+07	-1.34E+06	-1.04E+05
6.00E+03	1.28E+11	1.84E+10	9.20E+09	1.24E+11	1.28E+10	1.84E+09	2.48E+08	4.52E+08	-1.86E+08	-7.76E+06	-3.64E+05
8.00E+03	2.10E+11	2.72E+10	9.94E+09	2.09E+11	2.10E+10	2.73E+09	3.47E+08	2.08E+09	2.18E+08	3.48E+07	5.08E+05
1.00E+04	3.13E+11	3.77E+10	1.13E+10	3.15E+11	3.13E+10	3.77E+09	4.60E+08	3.17E+09	3.16E+08	3.13E+07	3.29E+06
1.50E+04	6.62E+11	7.11E+10	1.59E+10	6.74E+11	6.62E+10	7.11E+09	8.09E+08	7.02E+09	6.89E+08	6.79E+07	6.77E+06
2.00E+04	1.14E+12	1.15E+11	2.14E+10	1.17E+12	1.14E+11	1.15E+10	1.25E+09	1.20E+10	1.21E+09	1.20E+08	1.18E+07
2.50E+04	1.76E+12	1.71E+11	2.76E+10	1.80E+12	1.76E+11	1.71E+10	1.79E+09	1.25E+10	1.83E+09	1.85E+08	1.83E+07
3.00E+04	2.51E+12	2.39E+11	3.47E+10	2.56E+12	2.51E+11	2.39E+10	2.44E+09	6.24E+10	2.44E+09	2.61E+08	2.62E+07
4.00E+04	4.43E+12	4.11E+11	5.09E+10	4.51E+12	4.43E+11	4.11E+10	4.05E+09	5.94E+10	8.68E+09	4.21E+08	4.52E+07
5.00E+04	6.89E+12	6.34E+11	7.01E+10	7.00E+12	6.89E+11	6.34E+10	6.11E+09	8.49E+10	8.88E+09	4.05E+08	6.78E+07

TABLE 6
Photoelectric Coefficient

T	1SC	2SC	3SC	1SE	2SE	3SE	4FM
5.00E+03	-4.41E+07	-6.79E+06	2.61E+06	-3.54E+08	-4.41E+07	-6.79E+06	-2.93E+06
6.00E+03	-5.05E+07	-7.30E+06	2.63E+06	-4.21E+08	-5.05E+07	-7.30E+06	-3.01E+06
8.00E+03	-6.33E+07	-8.34E+06	3.04E+06	-5.55E+08	-6.33E+07	-8.34E+06	-3.17E+06
1.00E+04	-7.62E+07	-9.41E+06	3.58E+06	-6.90E+08	-7.62E+07	-9.41E+06	-3.37E+06
1.50E+04	-1.09E+08	-1.22E+07	4.87E+06	-1.03E+09	-1.09E+08	-1.22E+07	-4.08E+06
2.00E+04	-1.42E+08	-1.52E+07	5.96E+06	-1.37E+09	-1.42E+08	-1.52E+07	-5.02E+06
2.50E+04	-1.76E+08	-1.84E+07	6.85E+06		-1.76E+08	-1.84E+07	-6.13E+06
3.00E+04	-2.09E+08	-2.15E+07	7.54E+06		-2.09E+08	-2.16E+07	-7.38E+06
4.00E+04	-2.76E+08	-2.80E+07	8.52E+06		-2.77E+08	-2.81E+07	-1.01E+07
5.00E+04	-2.93E+08	-3.48E+07	9.03E+06			-3.47E+07	-1.30E+07

TABLE 7
Photoambipolar Coefficient

T	1SC	2SC	3SC	1SE	2SE	3SE	4FM
5.00E+03	5.93E+10	5.48E+09	1.54E+09	6.53E+10	5.93E+09	5.49E+08	5.92E+07
6.00E+03	8.29E+10	7.49E+09	1.65E+09	9.02E+10	8.29E+09	7.50E+08	7.90E+07
8.00E+03	1.41E+11	1.24E+10	2.12E+09	1.51E+11	1.41E+10	1.24E+09	1.27E+08
1.00E+04	2.14E+11	1.85E+10	2.75E+09	2.24E+11	2.14E+10	1.85E+09	1.85E+08
1.50E+04	4.60E+11	3.92E+10	4.78E+09	4.62E+11	4.60E+10	3.92E+09	3.80E+08
2.00E+04	7.96E+11	6.77E+10	7.41E+09	7.78E+11	7.96E+10	6.77E+09	6.43E+08
2.50E+04	1.22E+12	1.04E+11	1.06E+10		1.22E+11	1.04E+10	9.77E+08
3.00E+04	1.73E+12	1.49E+11	1.44E+10		1.73E+11	1.49E+10	1.38E+09
4.00E+04	3.01E+12	2.62E+11	2.35E+10		3.02E+11	2.62E+10	2.42E+09
5.00E+04		4.09E+11	3.50E+10			4.09E+10	3.75E+09

TABLE 8
Photothermal Coefficient

T	1SC	2SC	3SC	1SE	2SE	3SE	4FM
5.00E+03	1.16E+07	2.26E+07	4.16E+07	-1.26E+07	1.16E+07	2.24E+07	2.32E+07
6.00E+03	1.44E+07	3.13E+07	4.73E+07	-2.44E+07	1.35E+07	3.12E+07	3.24E+07
8.00E+03	1.51E+07	5.30E+07	6.58E+07	-4.62E+07	1.90E+07	5.19E+07	5.46E+07
1.00E+04	1.98E+07	7.74E+07	9.08E+07	-1.43E+08	1.62E+07	7.75E+07	8.14E+07
1.50E+04	2.51E+06	1.57E+08	1.73E+08	-7.80E+08	3.54E+07	1.64E+08	1.67E+08
2.00E+04	-1.22E+08	2.63E+08	2.84E+08	-1.97E+09	-4.01E+07	2.55E+08	2.89E+08
2.50E+04	-7.05E+07	3.73E+08	4.12E+08		-1.05E+08	3.87E+08	4.19E+08
3.00E+04	-3.09E+08	4.01E+08	5.86E+08		-5.80E+08	4.91E+08	6.05E+08
4.00E+04	-1.72E+09	2.73E+08	8.98E+08		-4.56E+08	5.80E+08	8.73E+08
5.00E+04		1.19E+09	1.29E+09			1.09E+09	1.67E+09

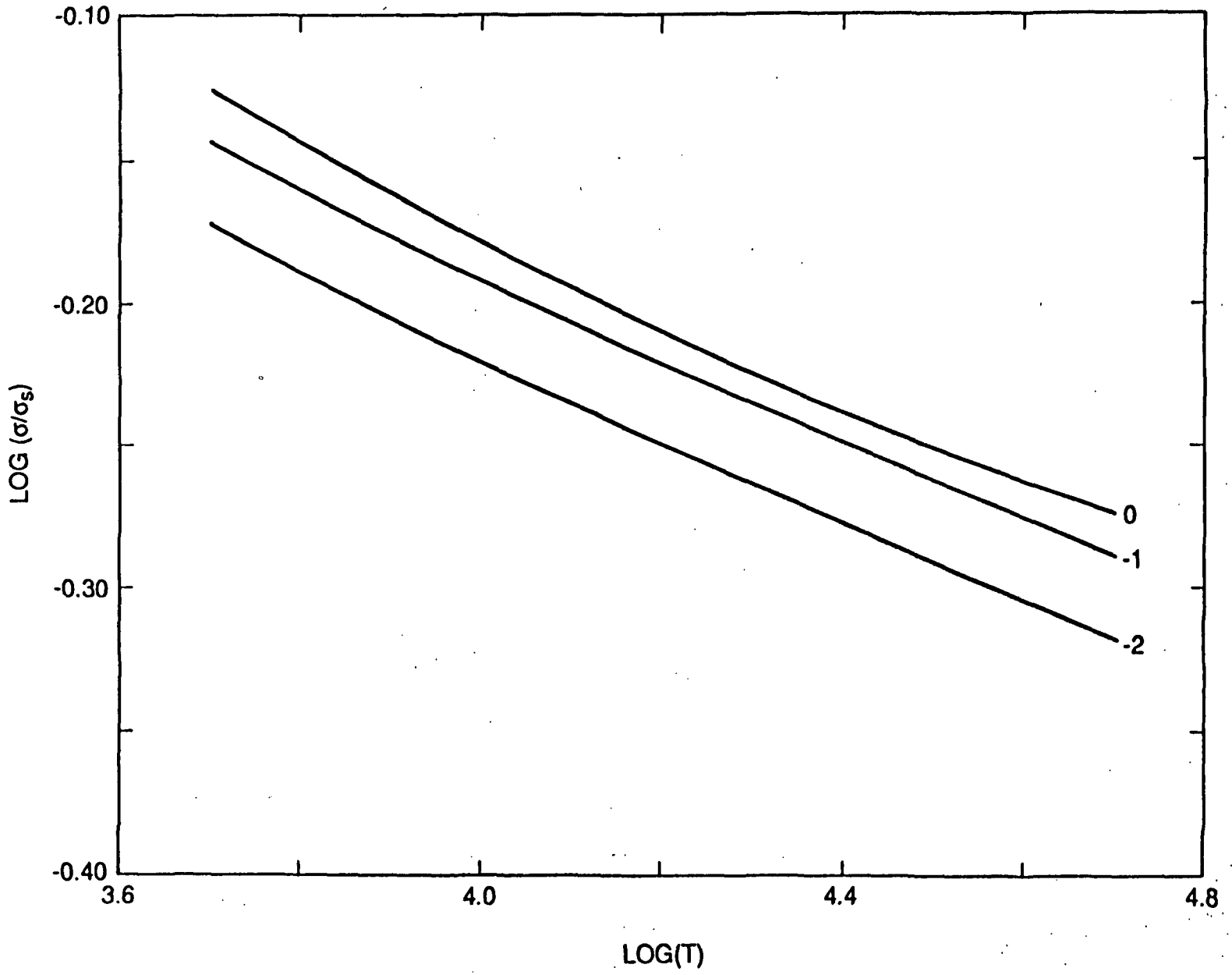

FIG. 1A

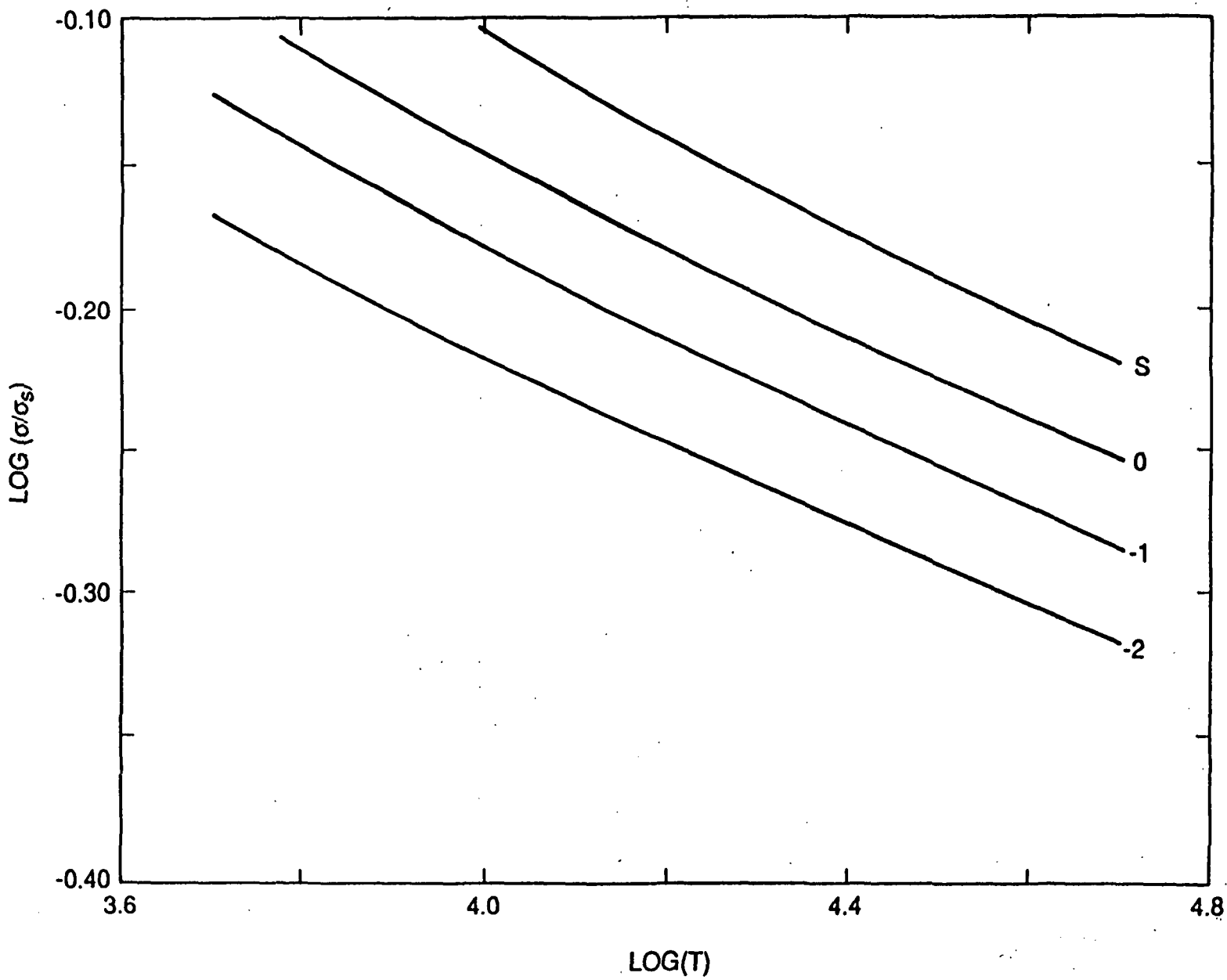

FIG. 1B

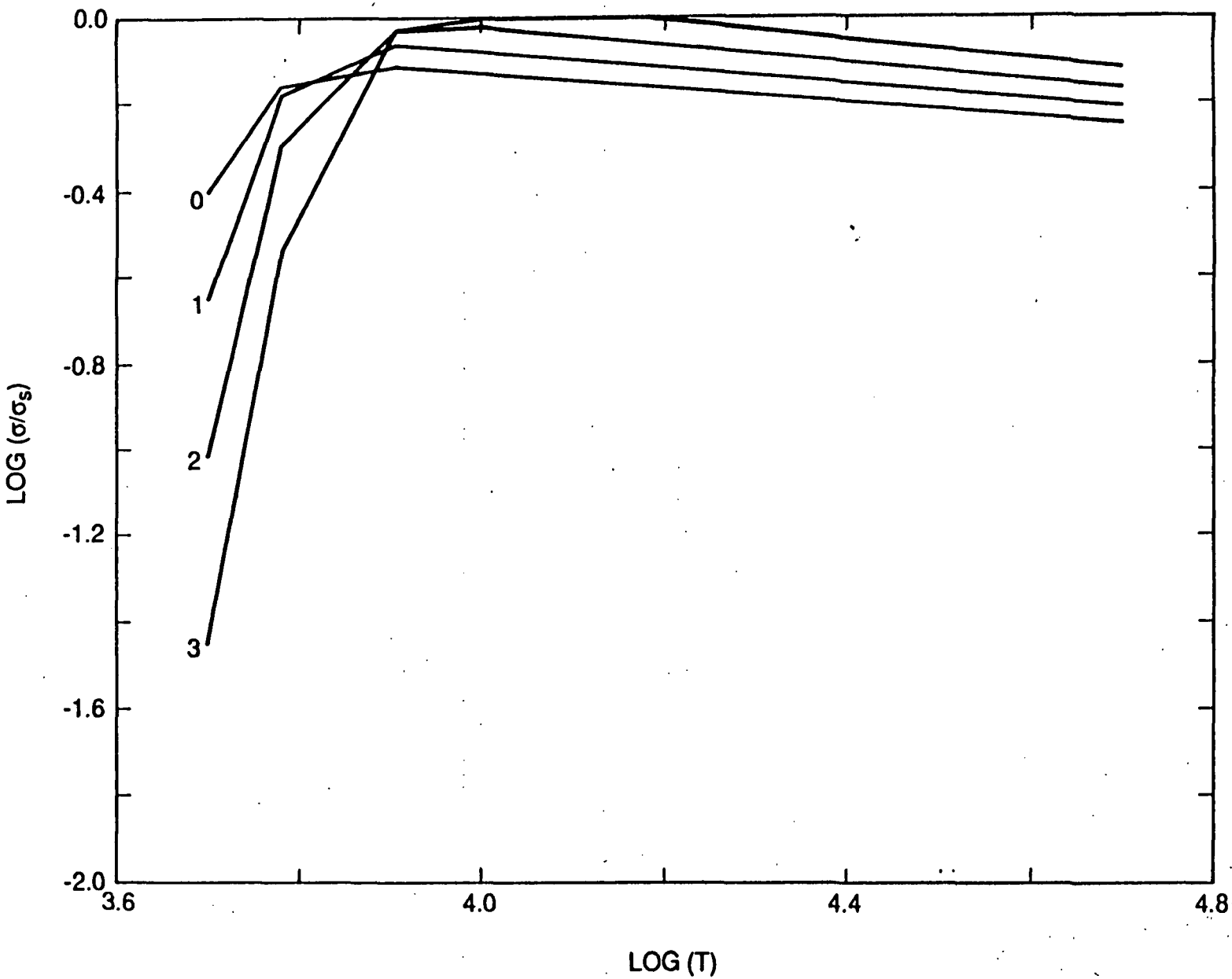

FIG. 1C

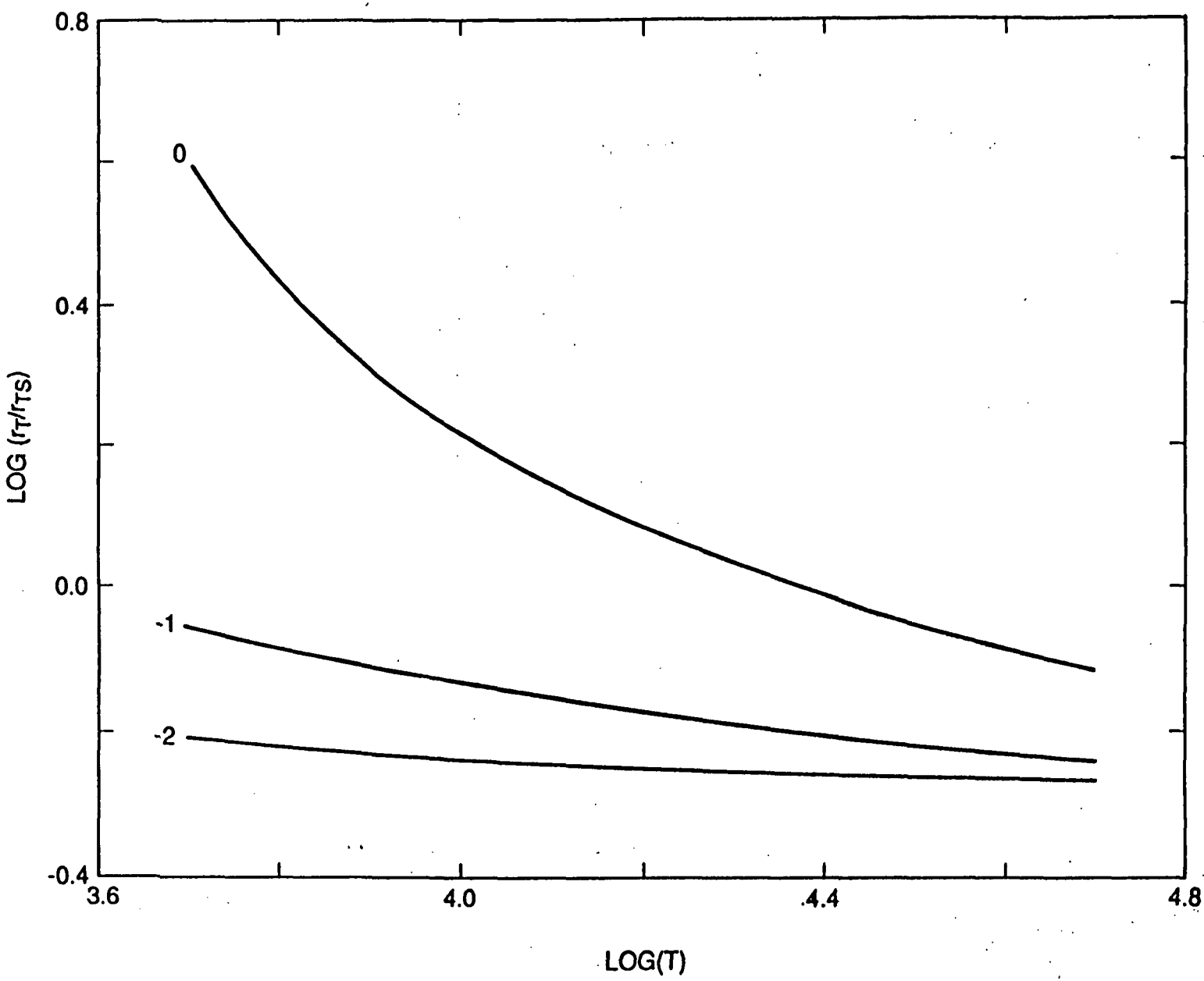

FIG. 2A

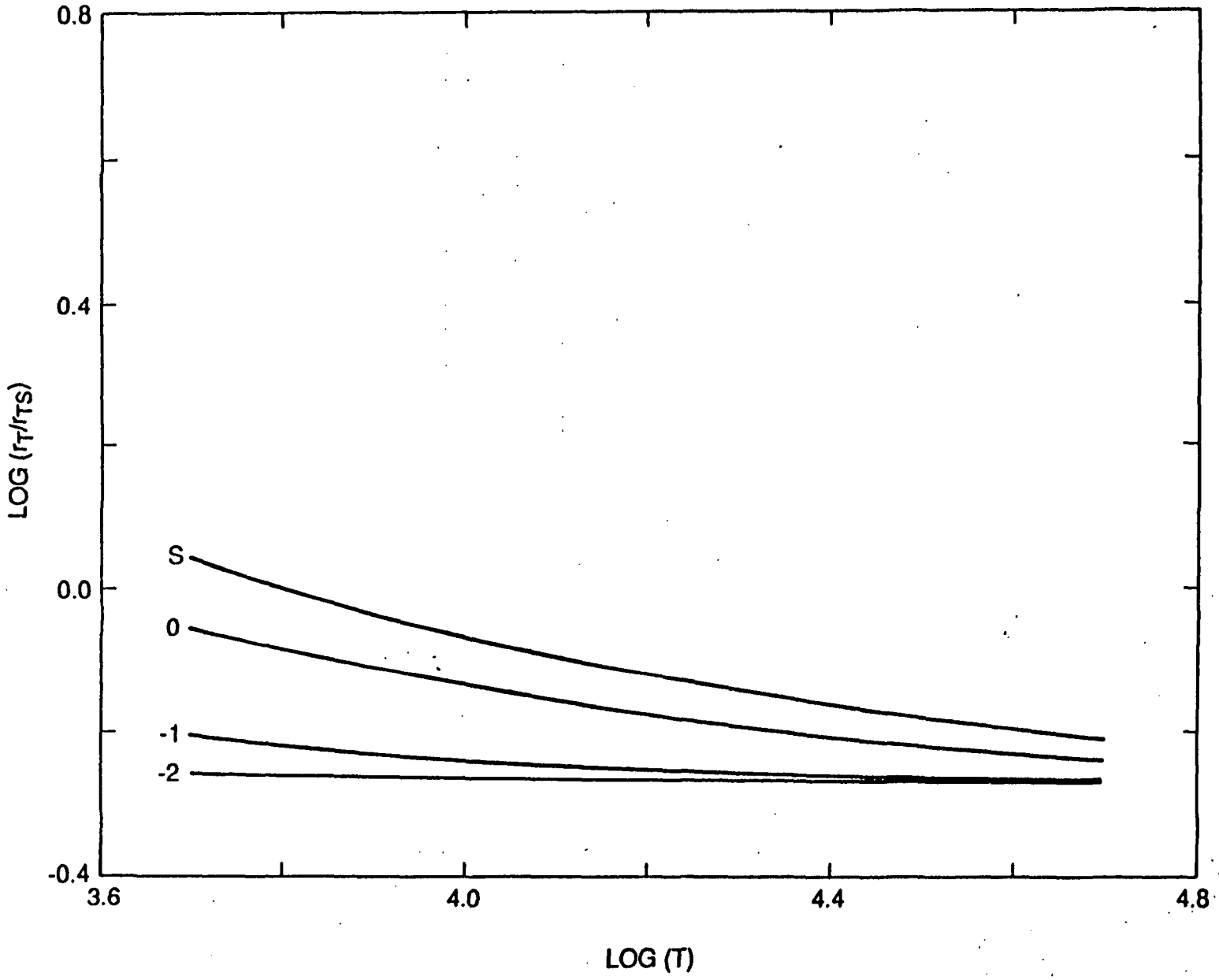

FIG. 2B

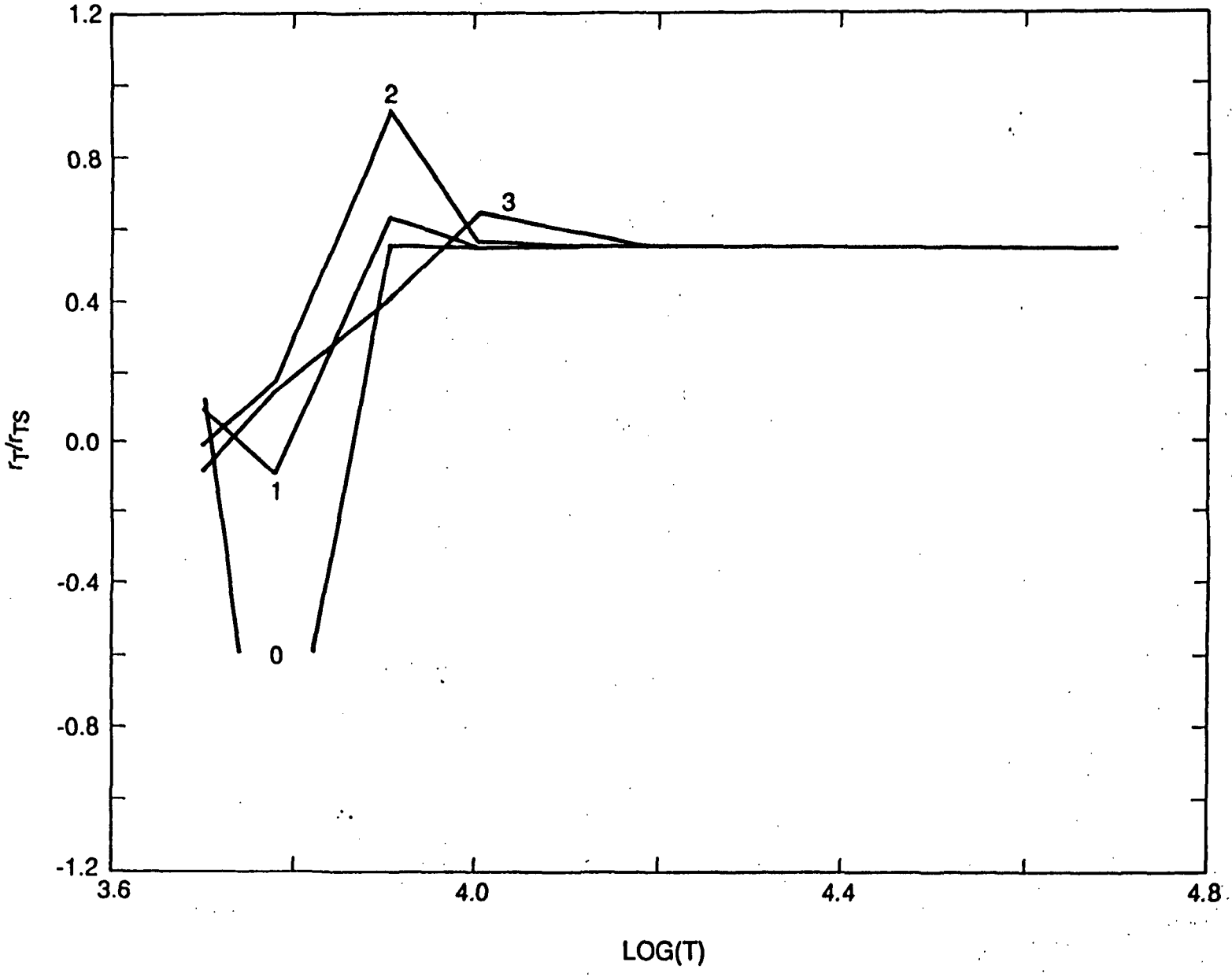

FIG. 2C

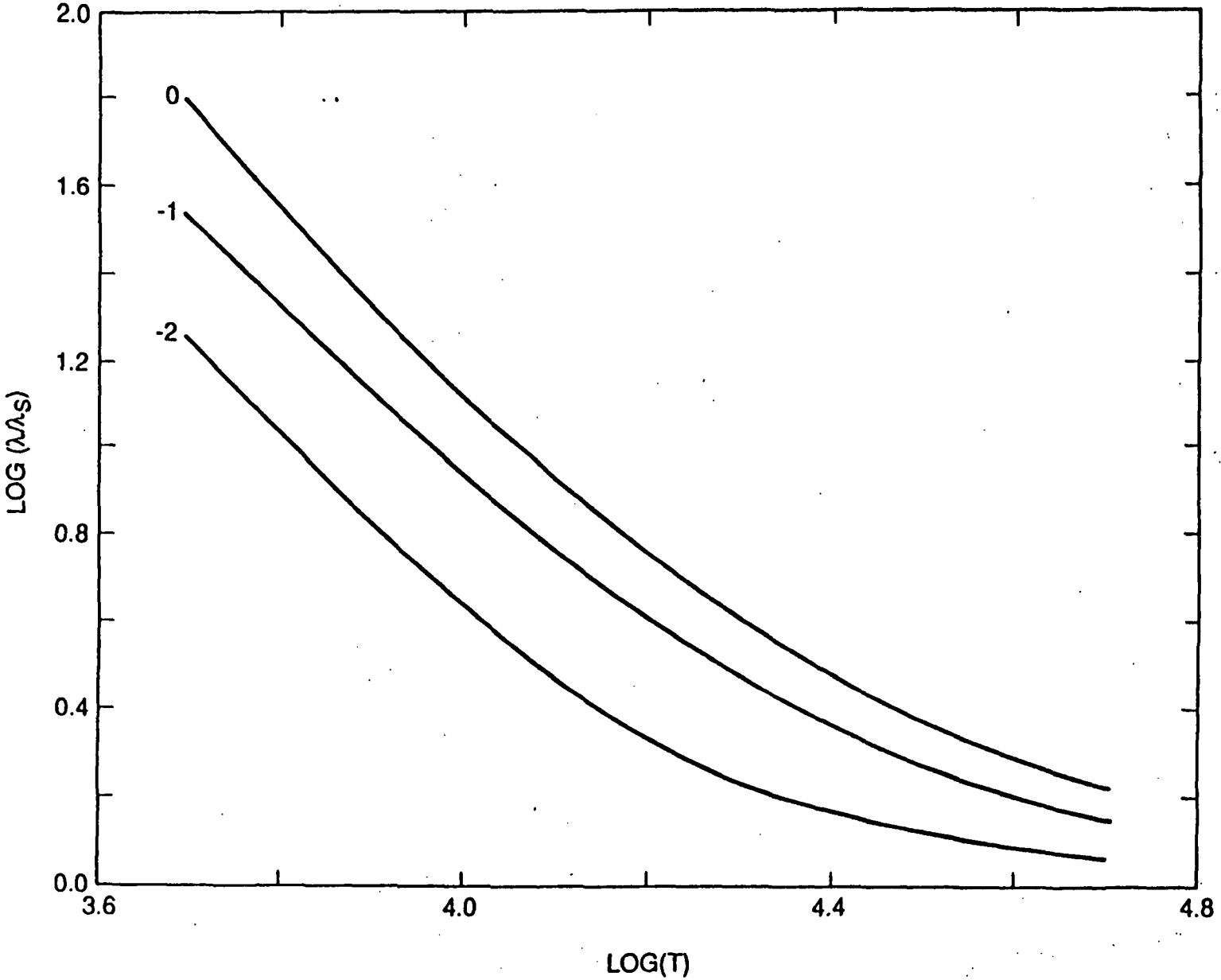

FIG. 3A

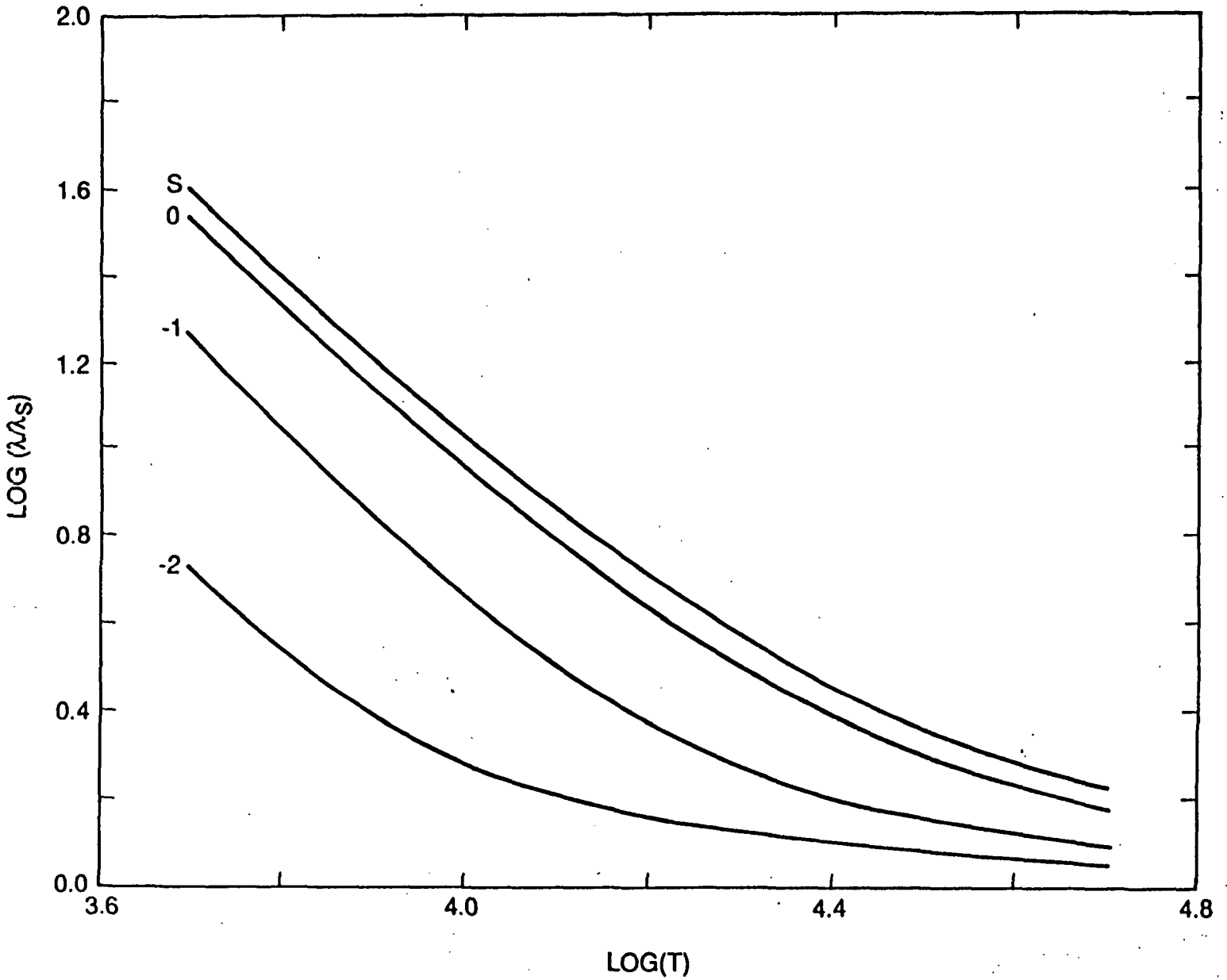

FIG. 3B

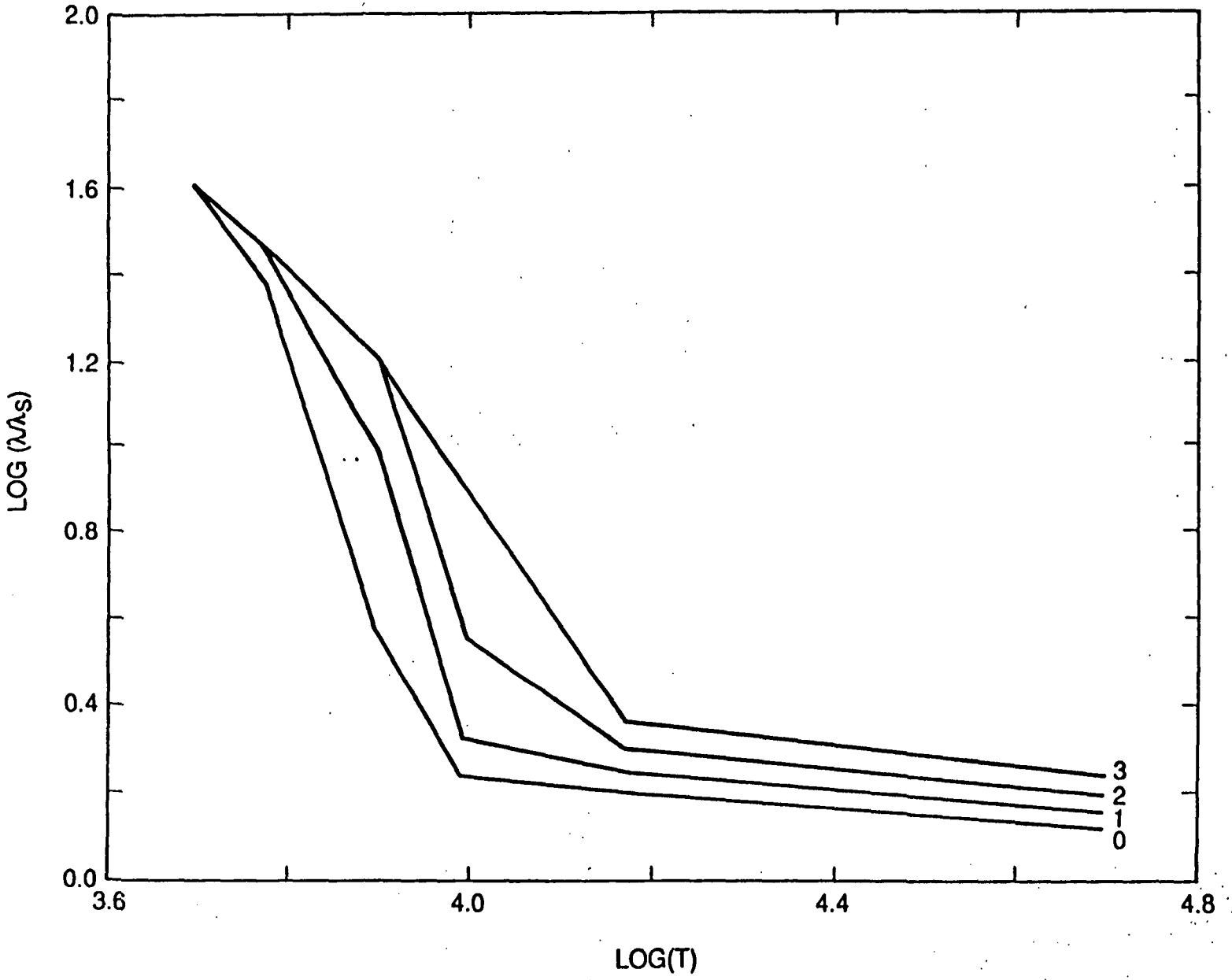

FIG. 3C

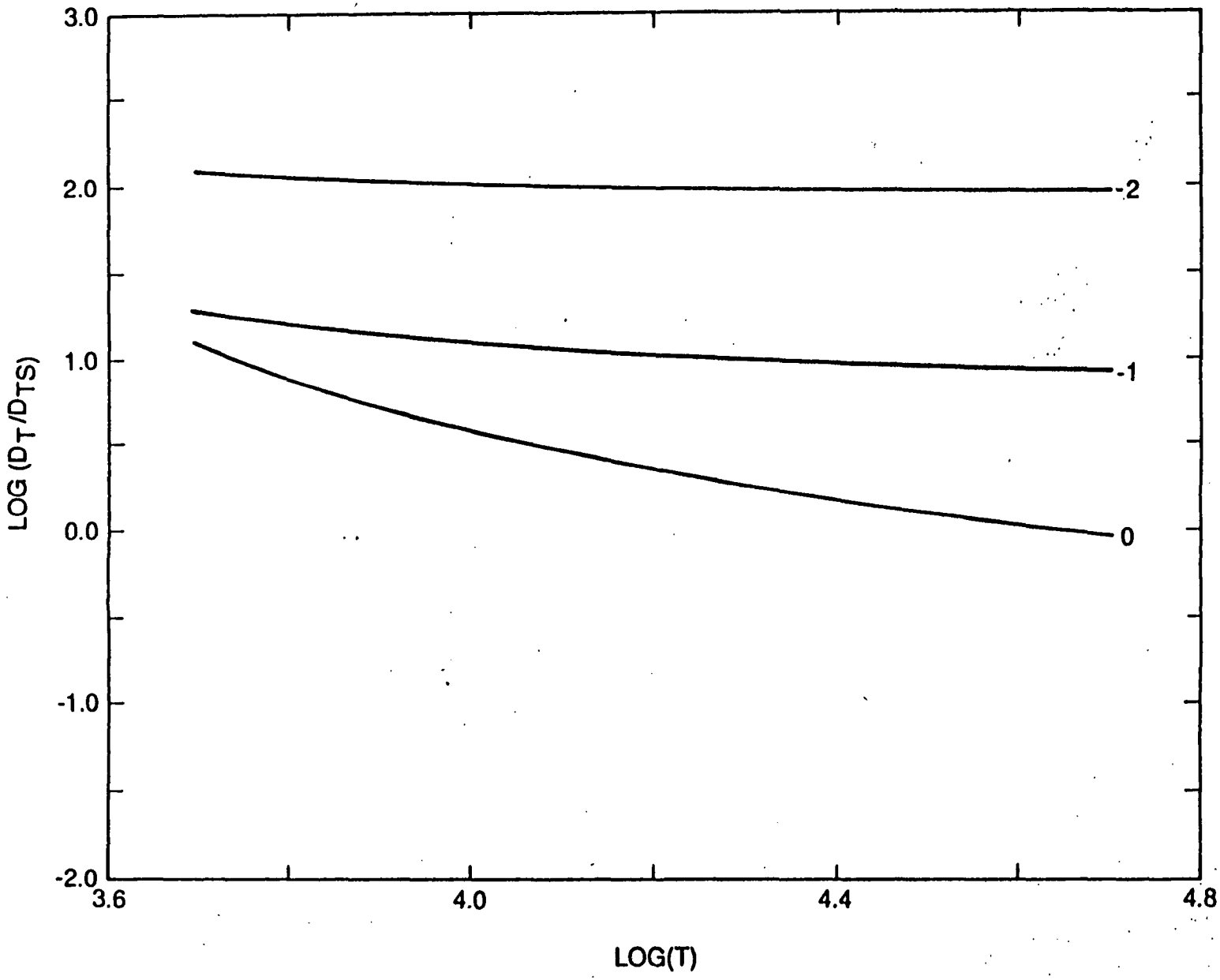

FIG. 4A

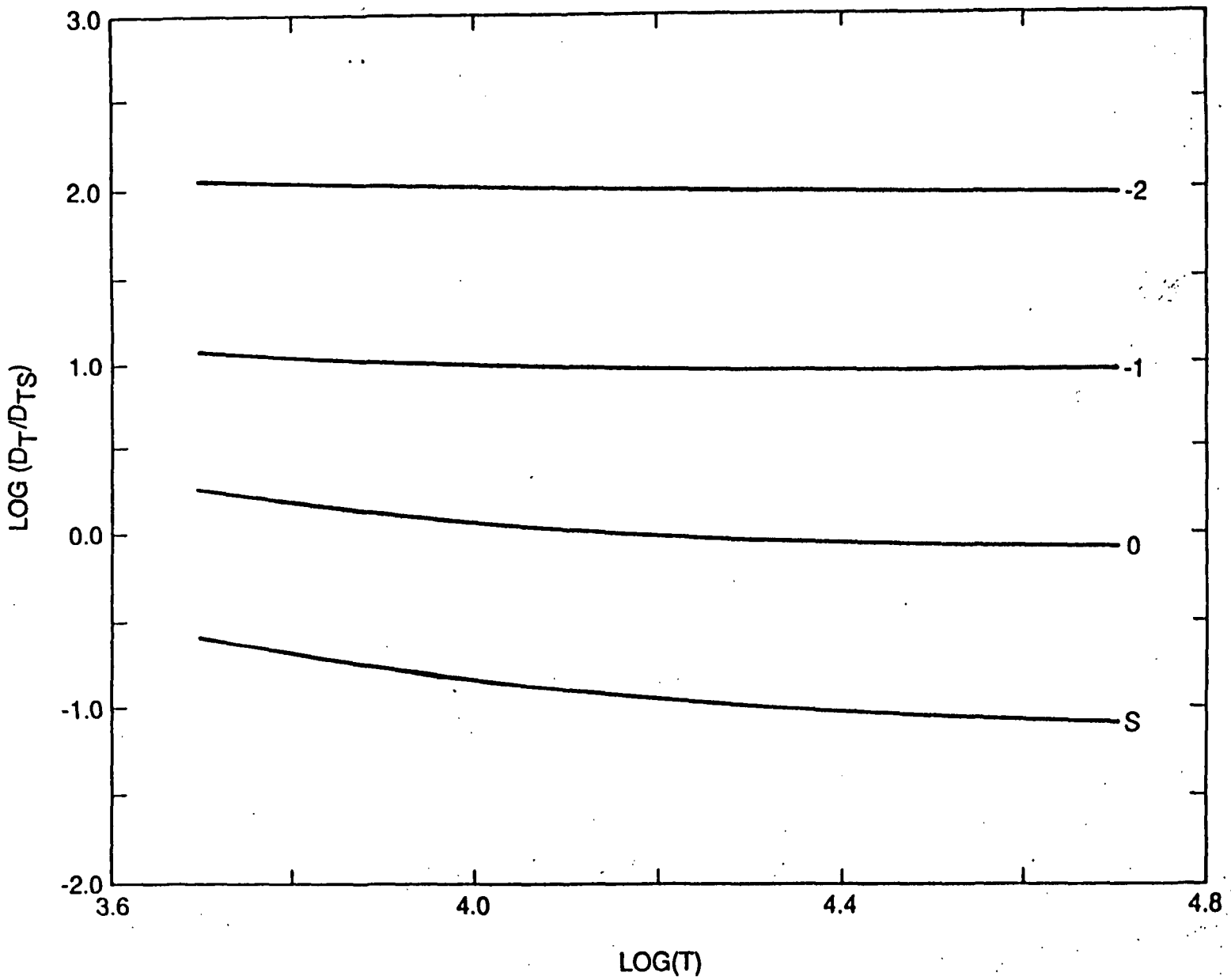

FIG. 4B

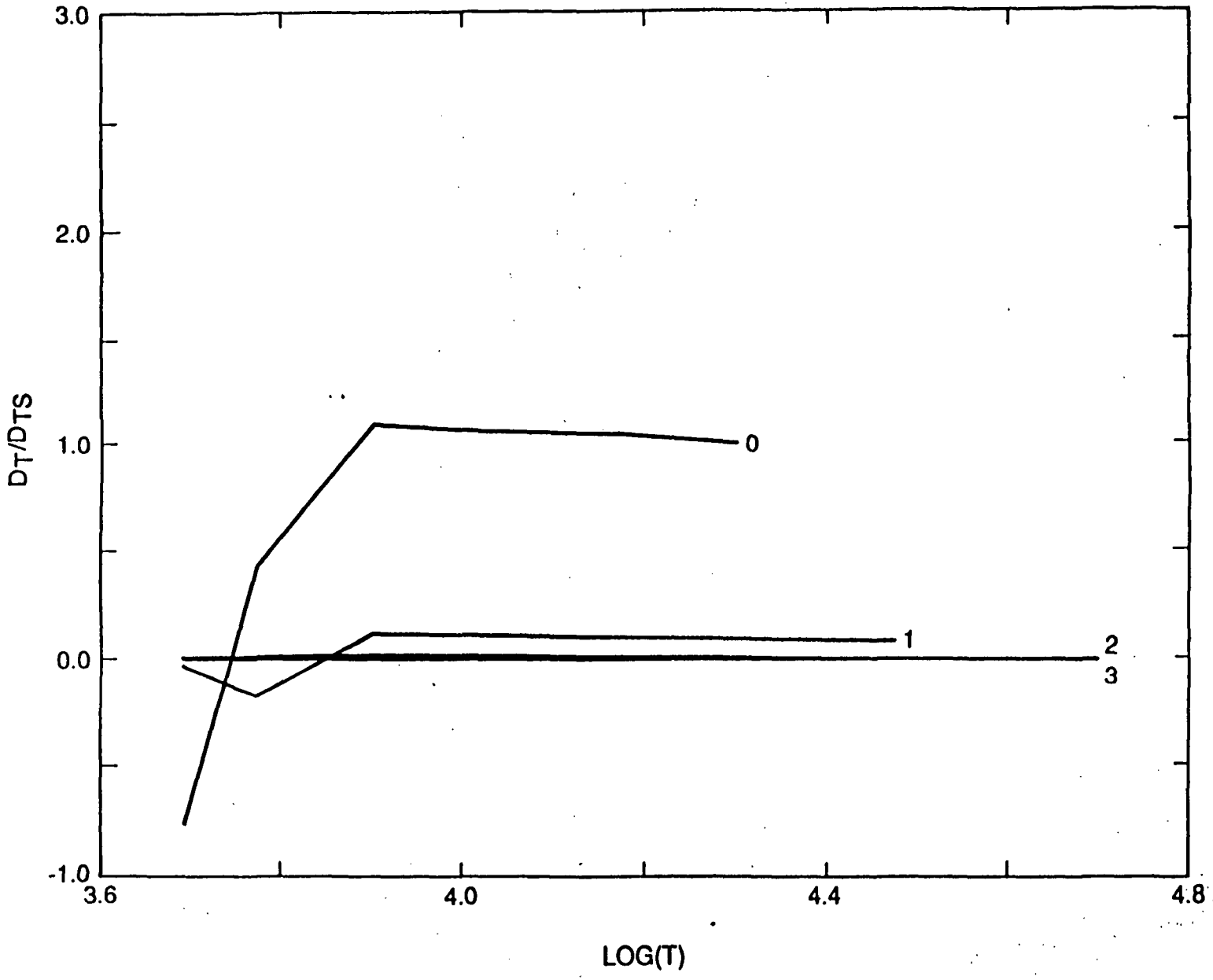

FIG. 4C

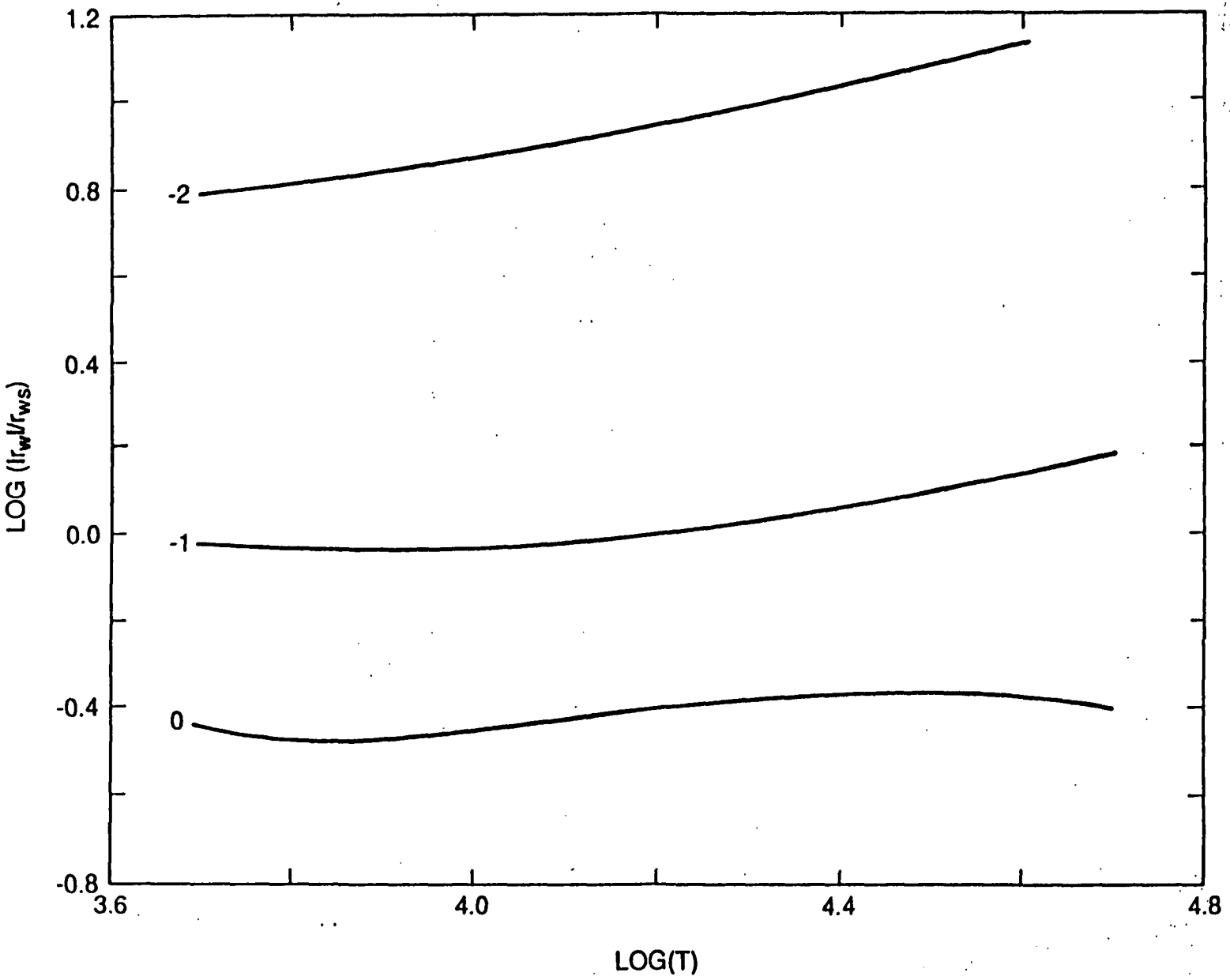

FIG. 5A

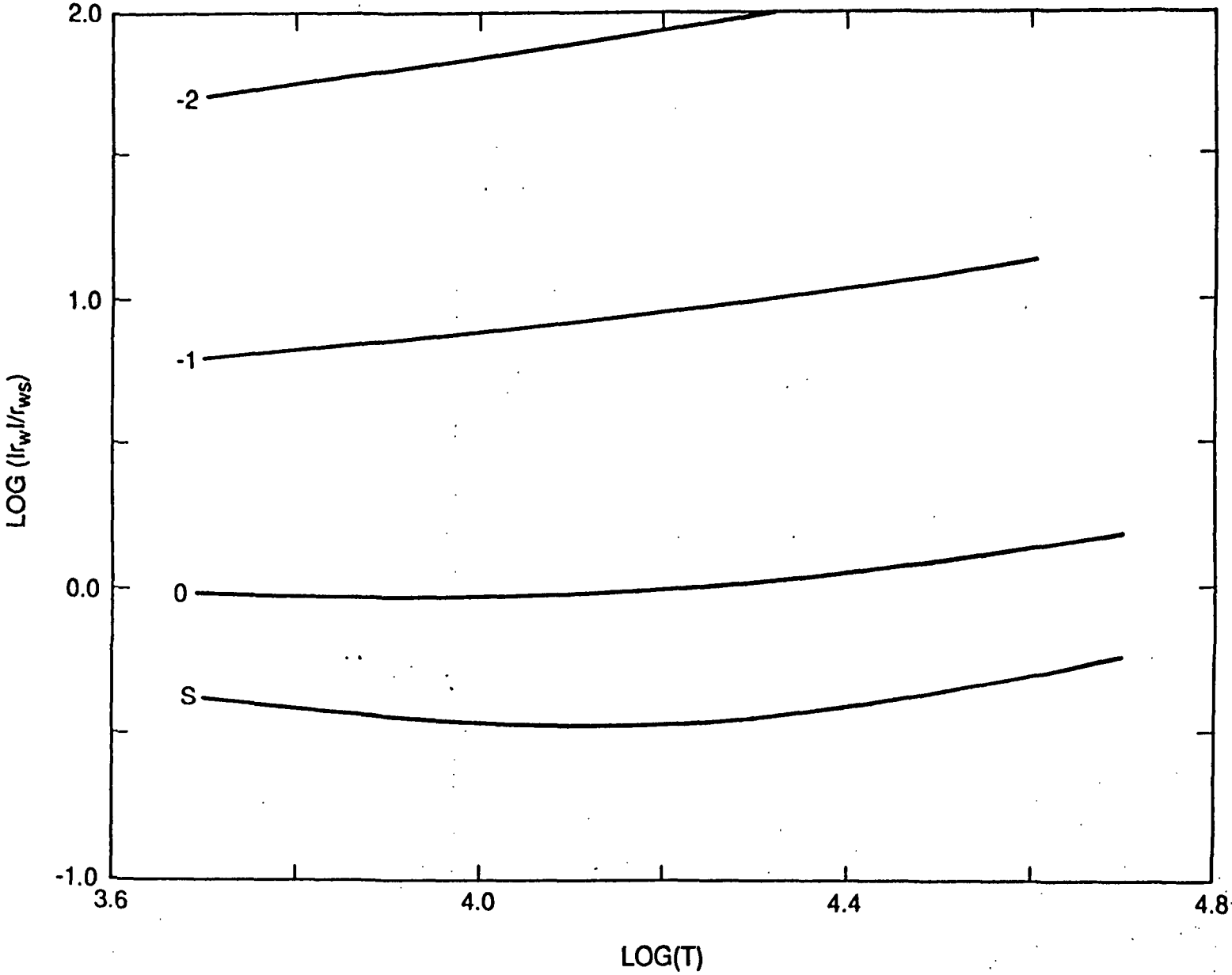

FIG. 5B

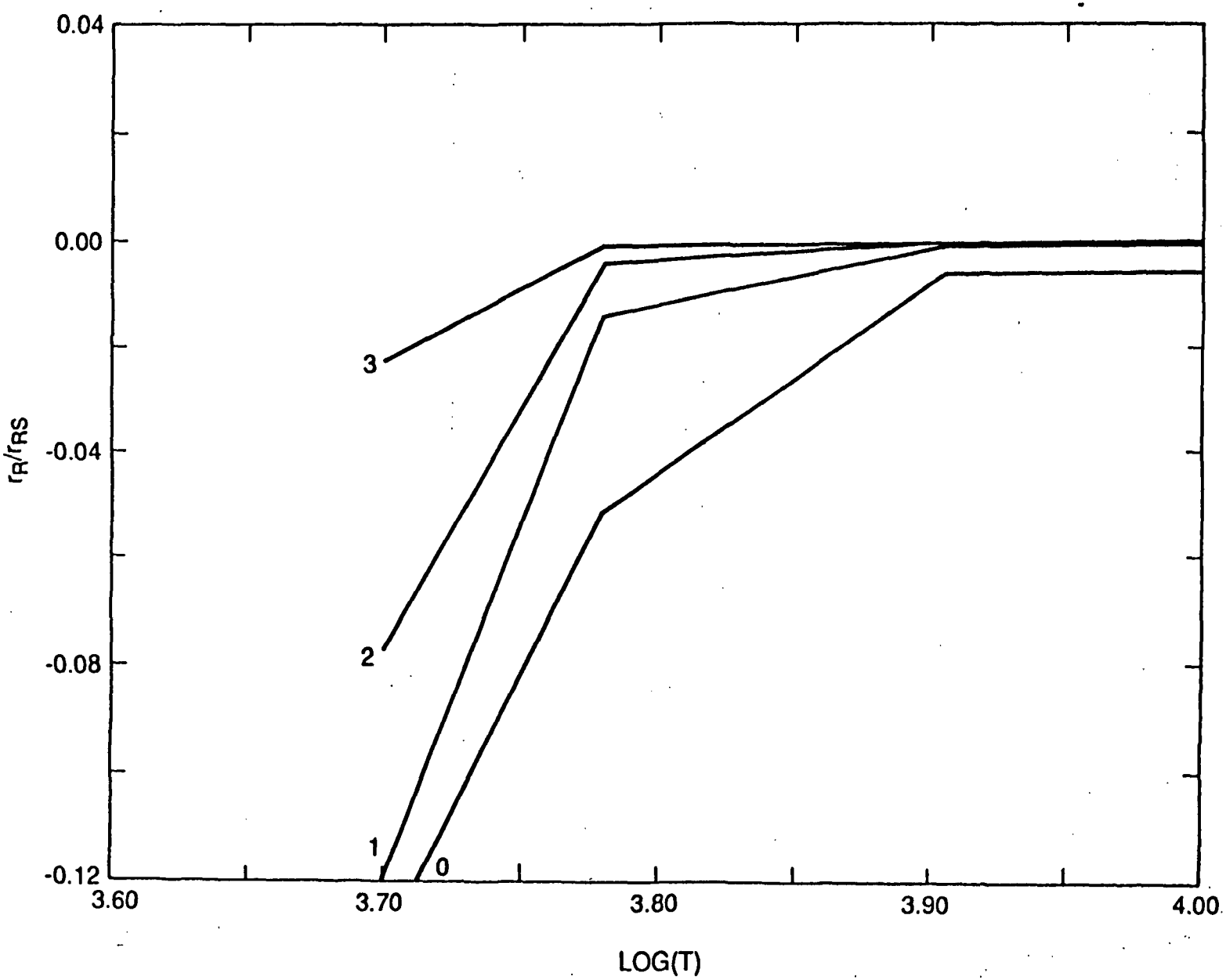

FIG. 5C

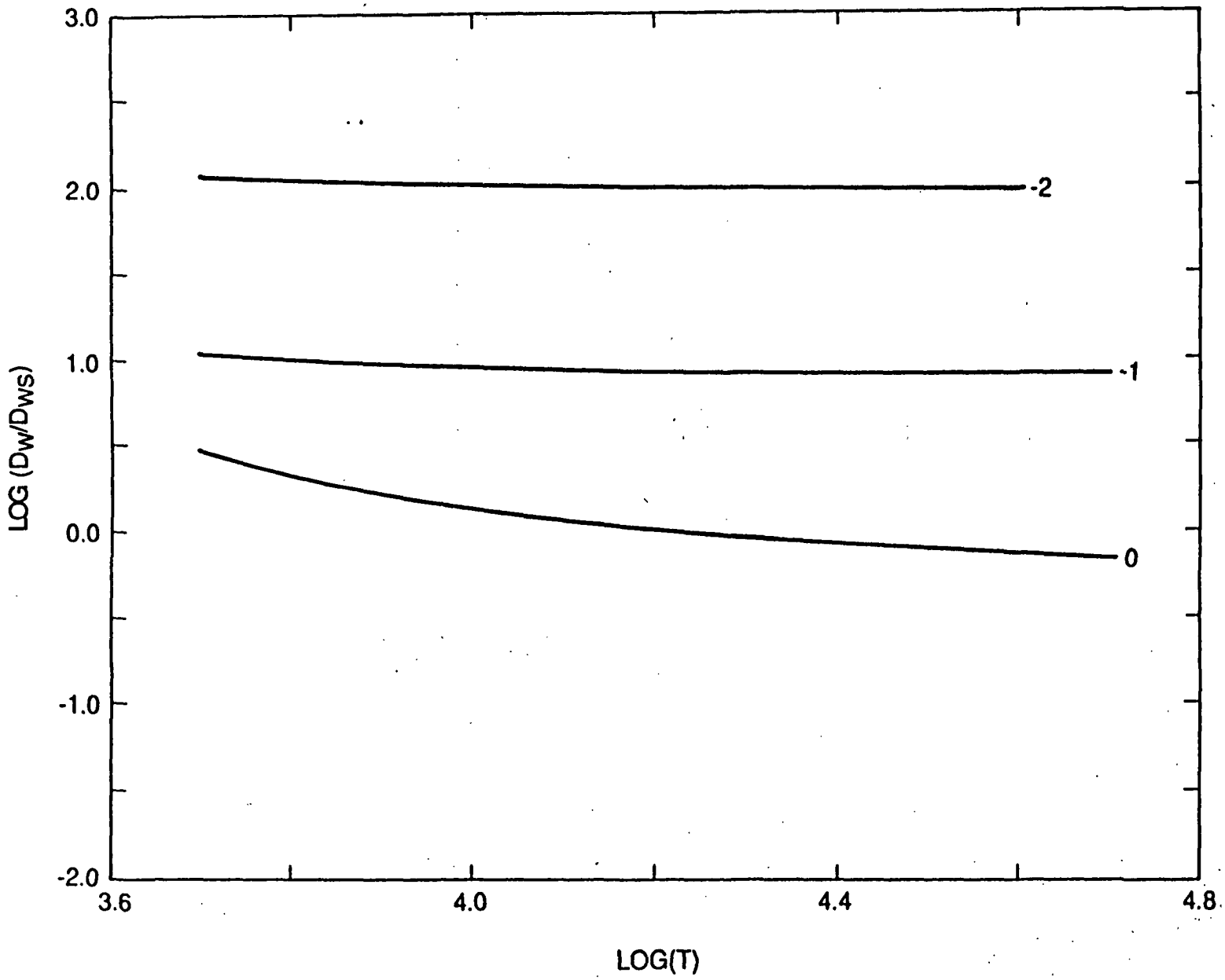

FIG. 6A

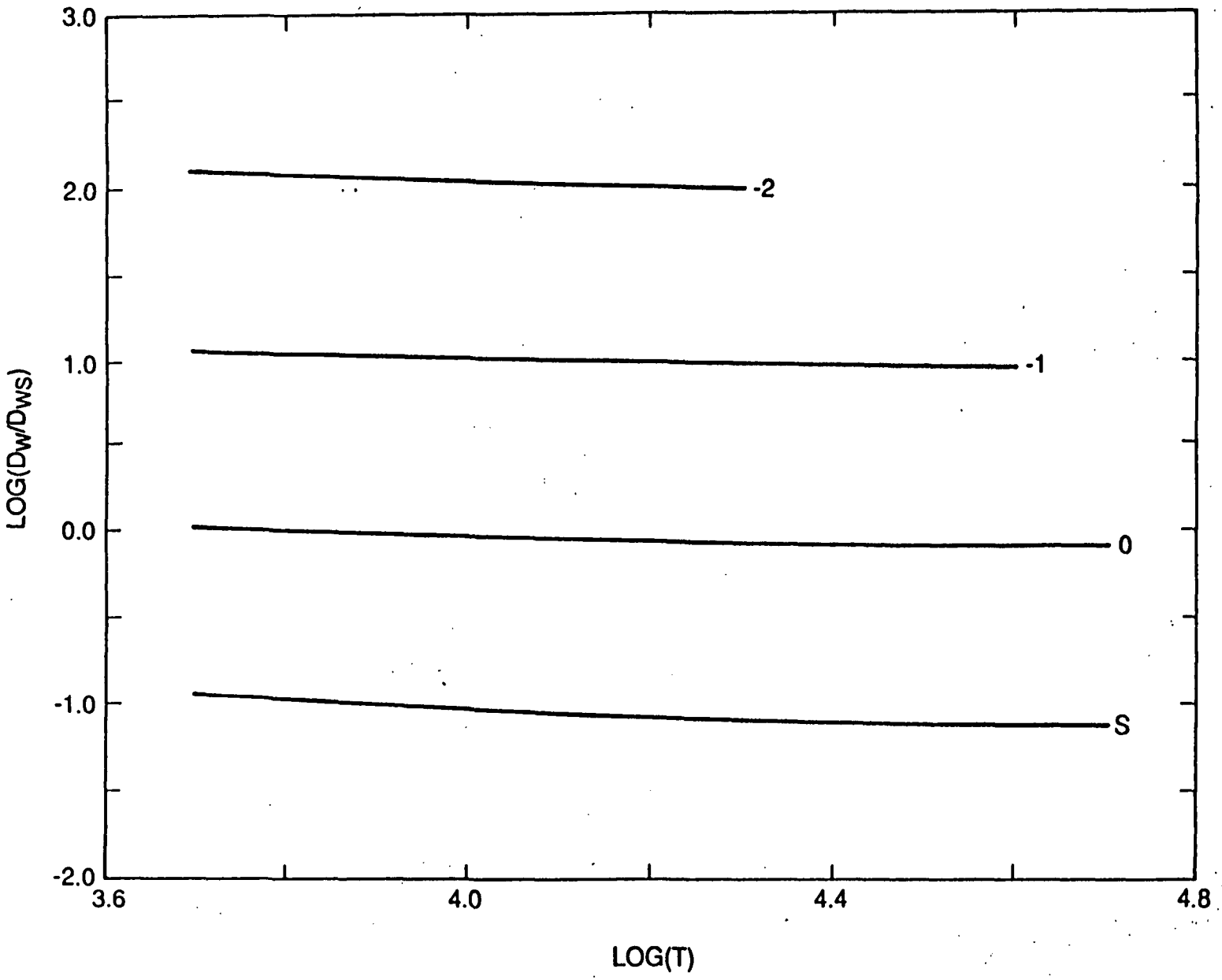

FIG. 6B

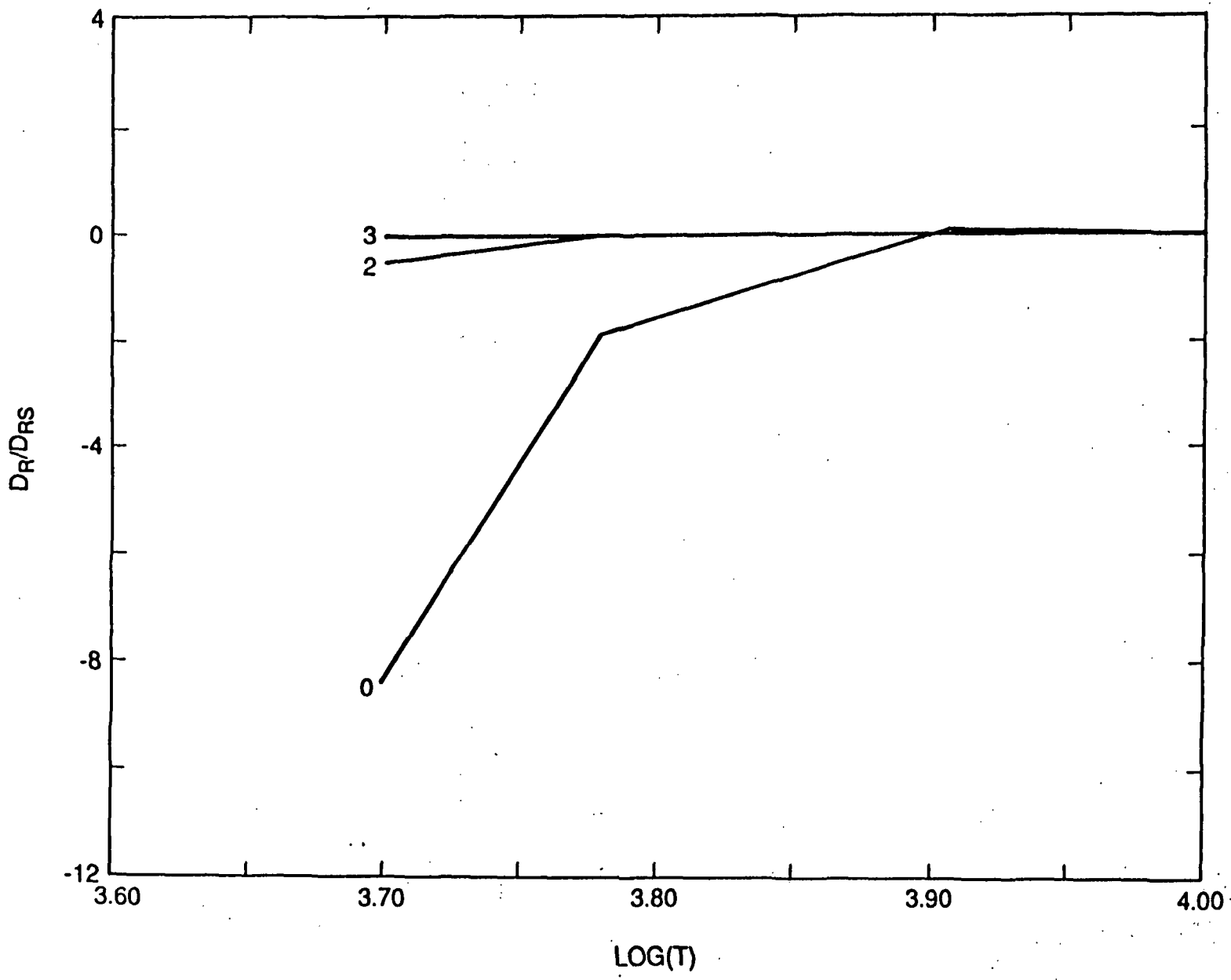

FIG. 6C

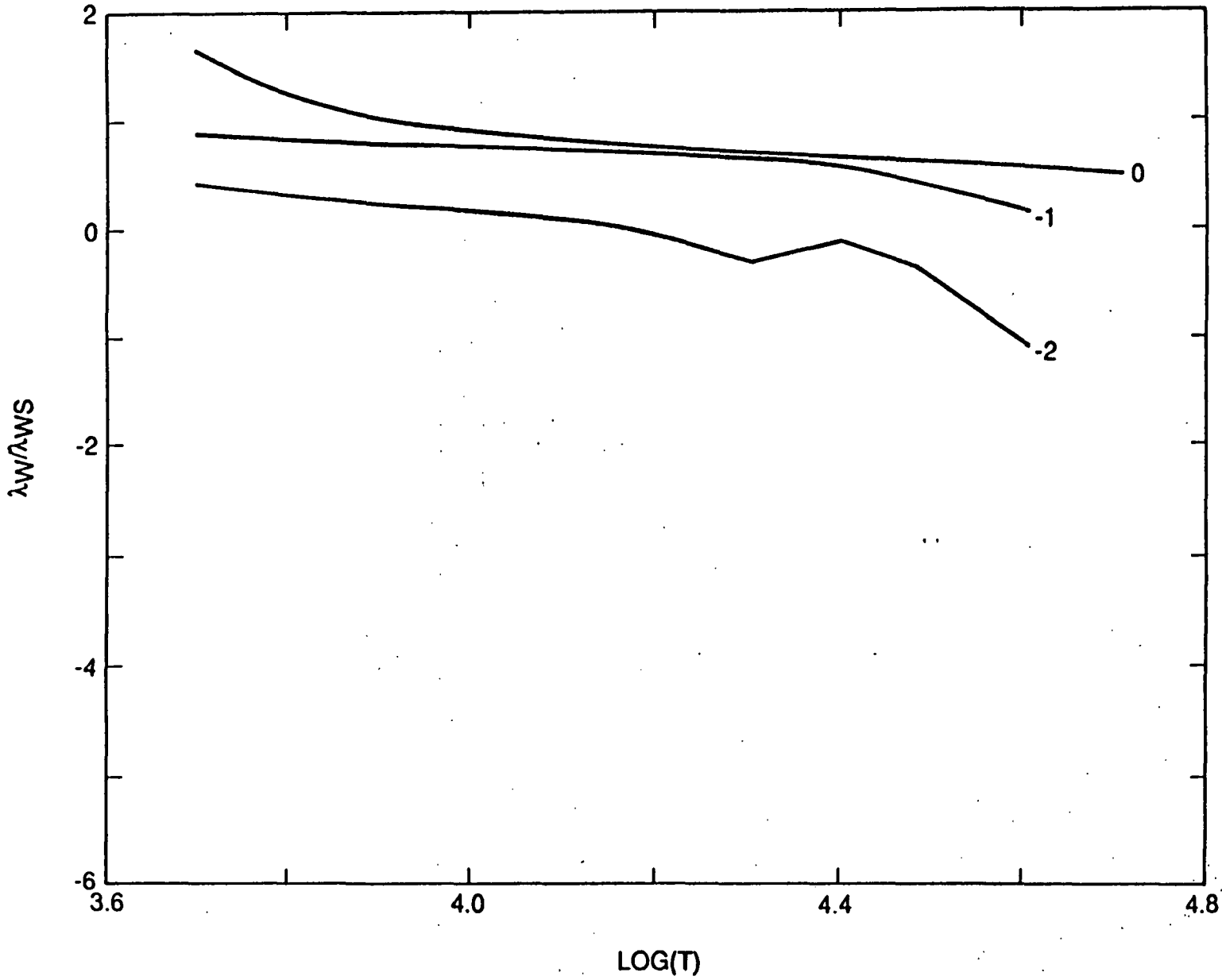

FIG. 7A

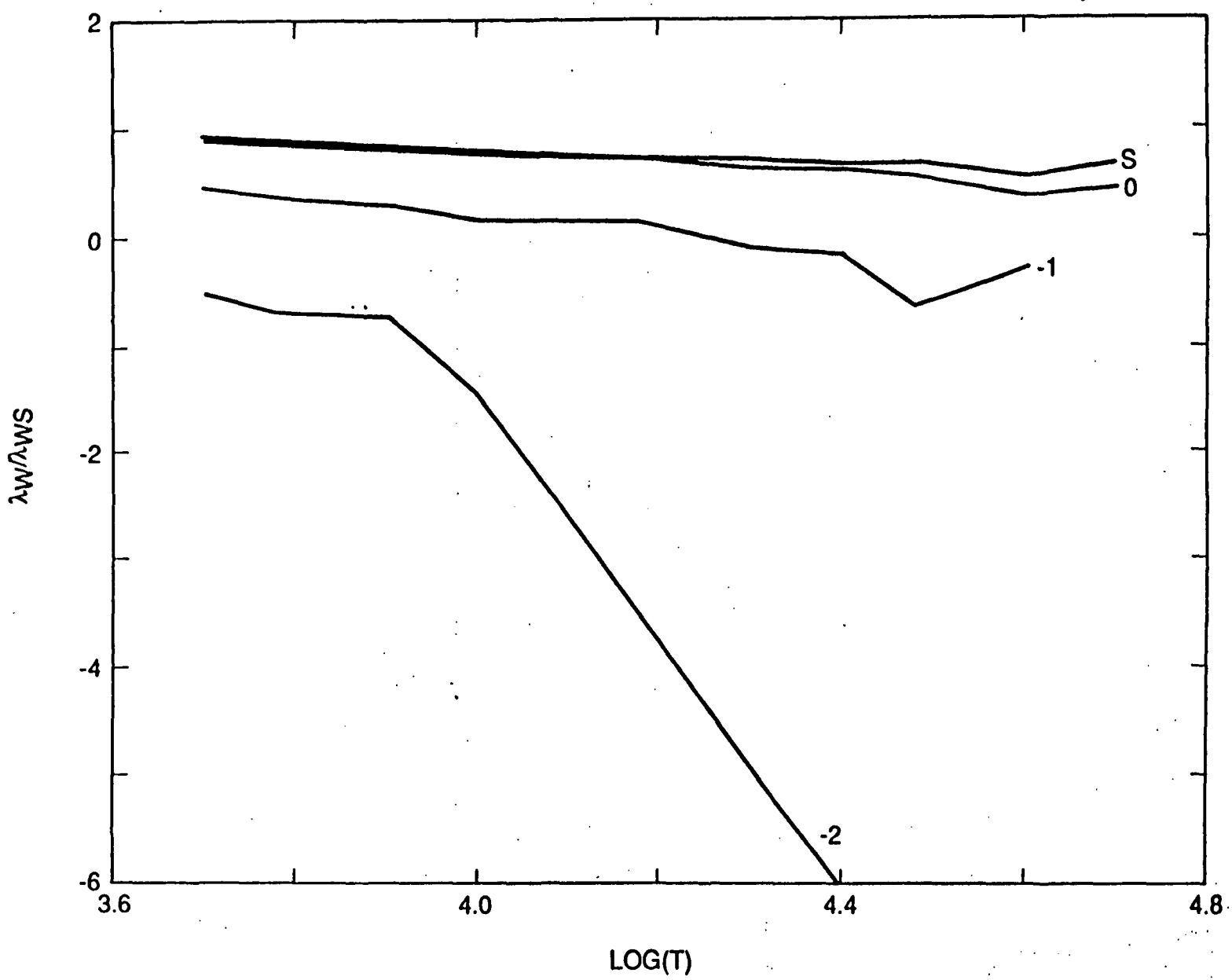

FIG 7B

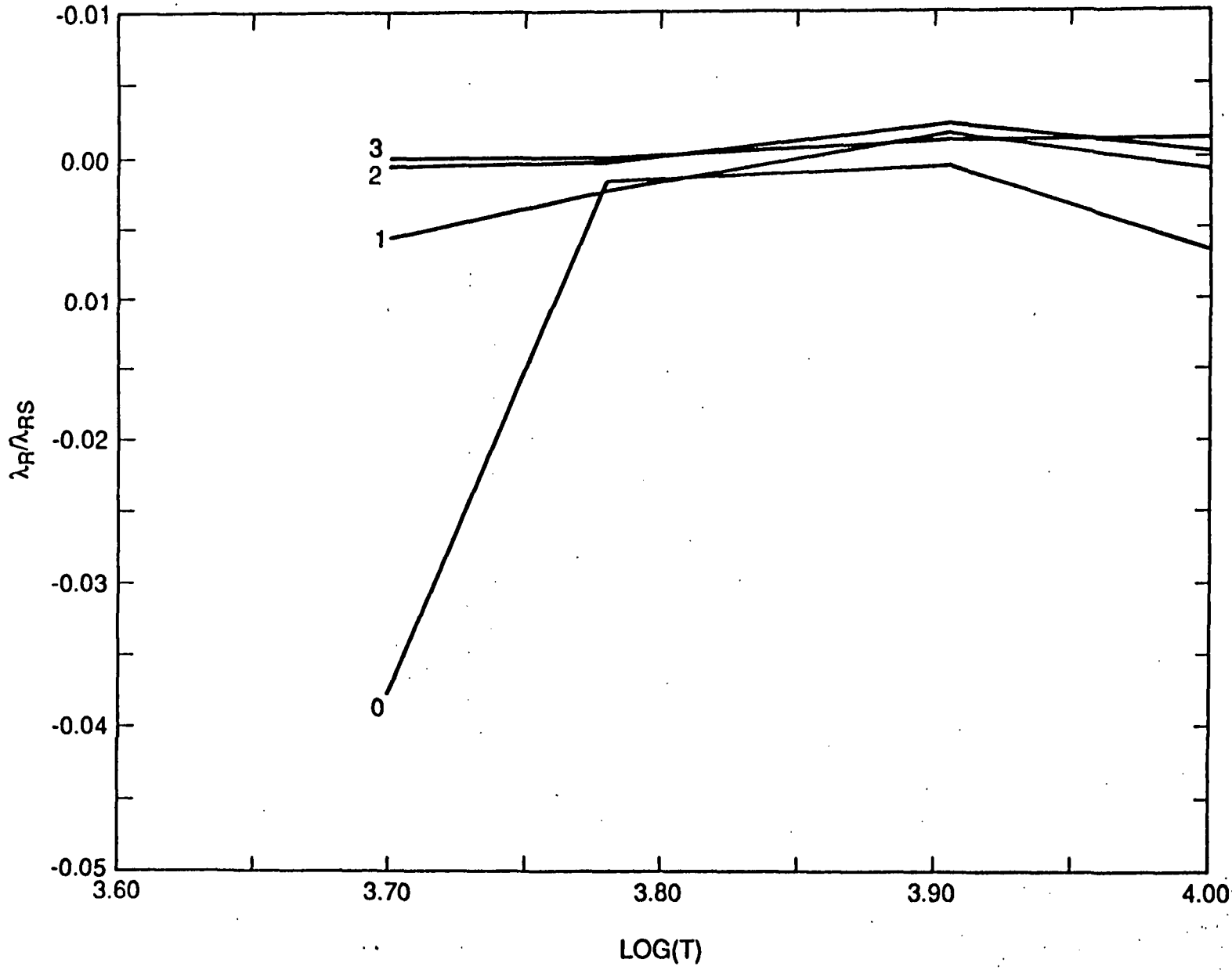
-0.01
0.00
0.01
-0.02
-0.03
-0.04
-0.05
λ_R/λ_{RS}
3
2
1
0
3.60
3.70
3.80
3.90
4.00
LOG(T)

FIG. 7C

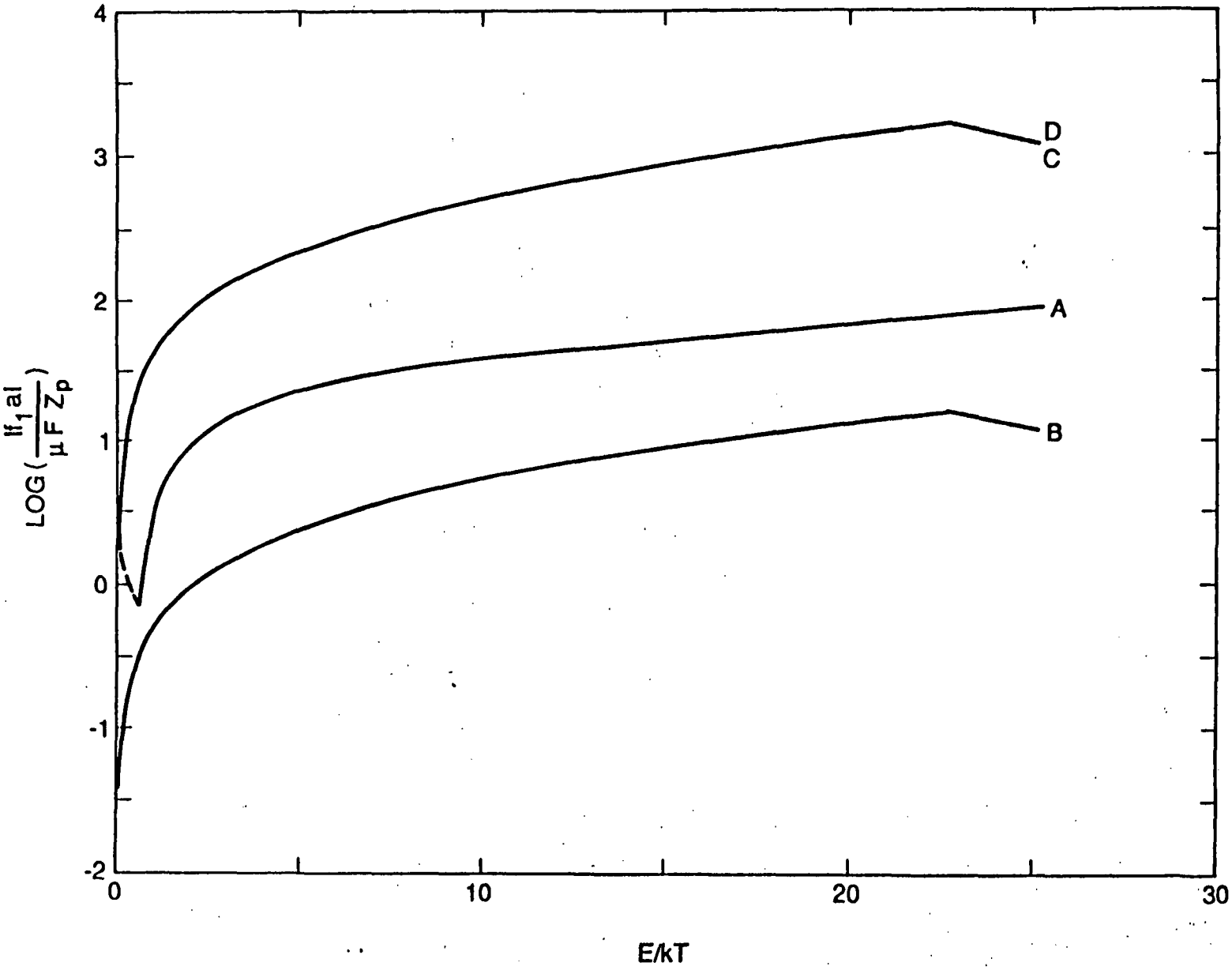

FIG. 8A

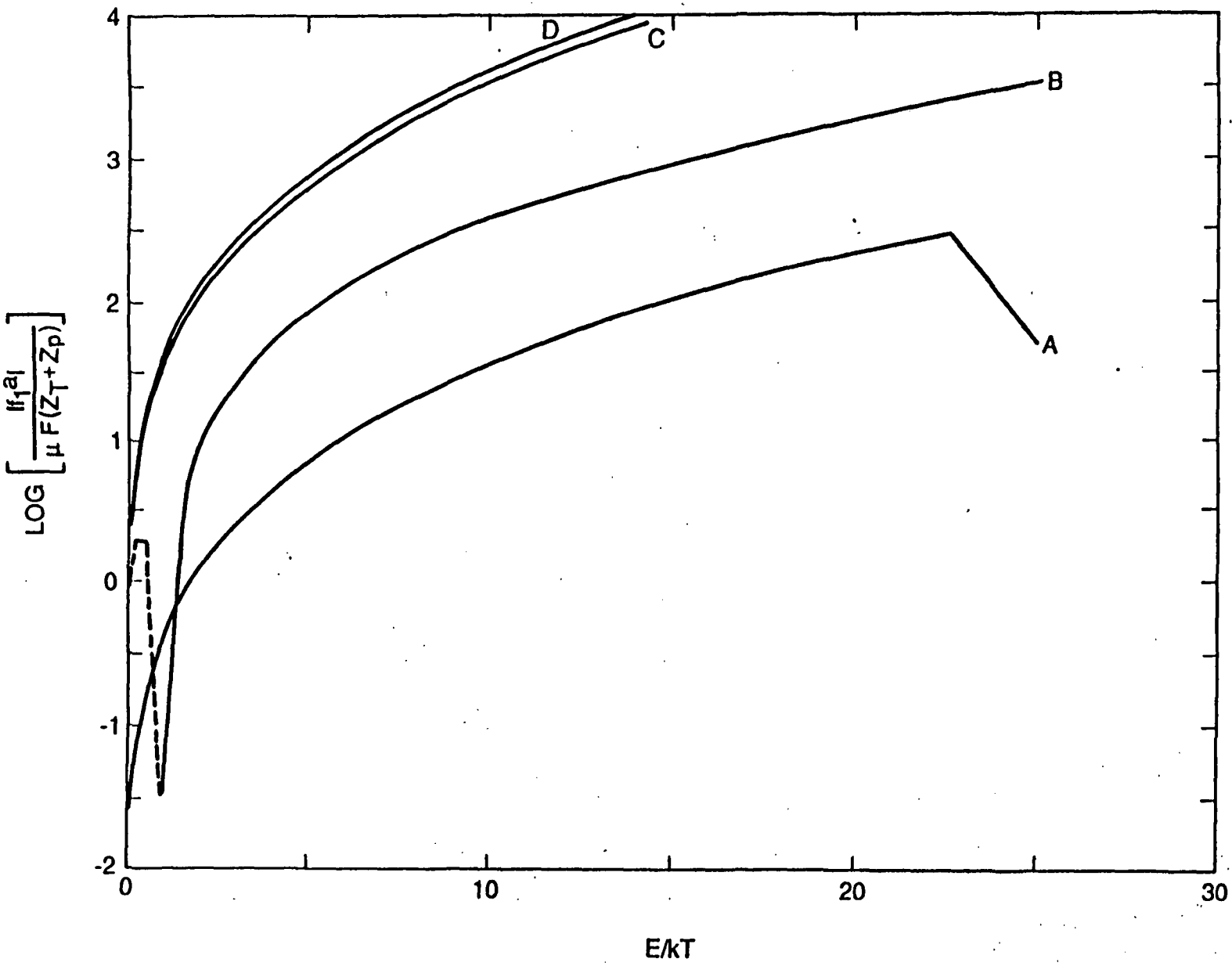

FIG. 8B

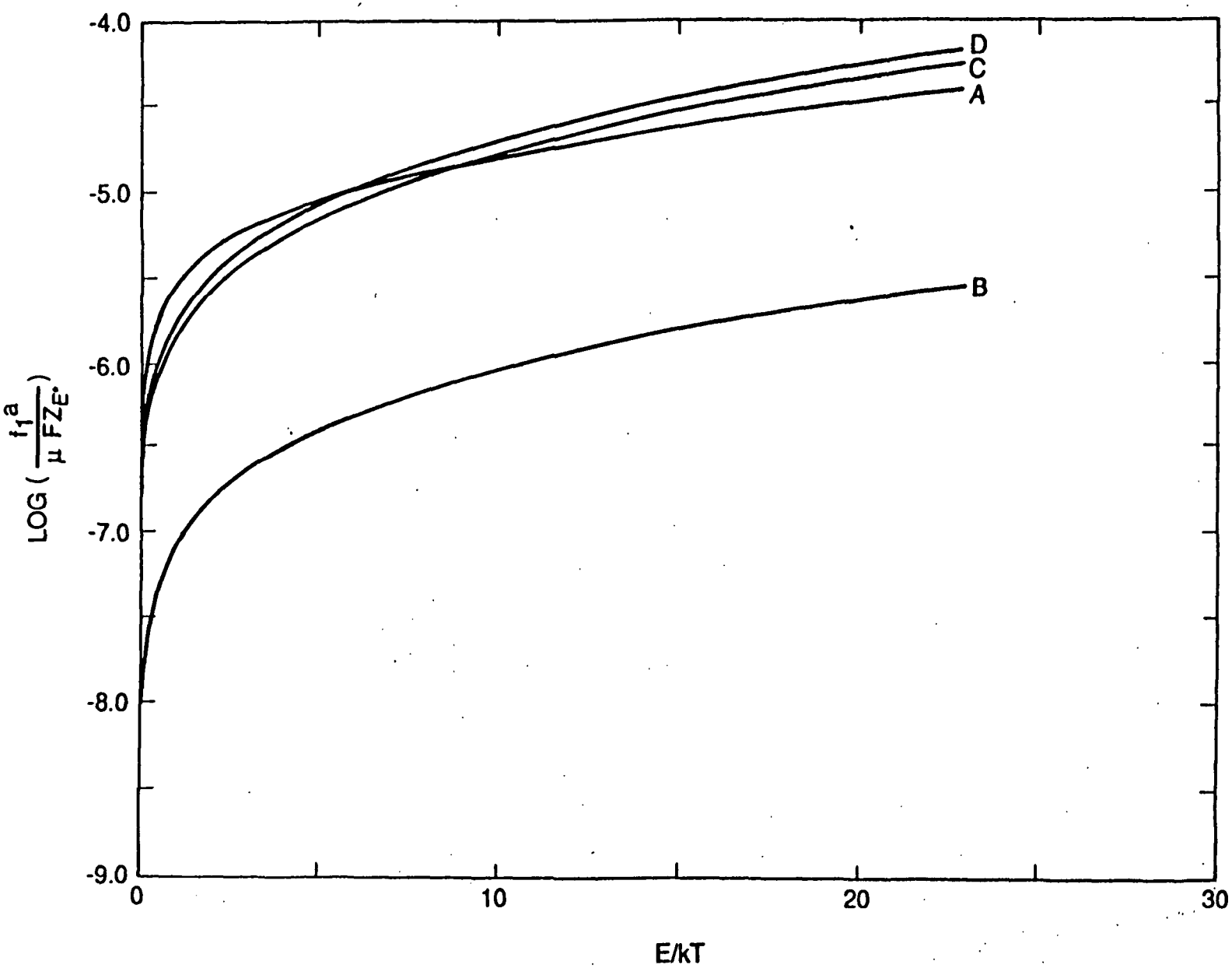

FIG. 8C

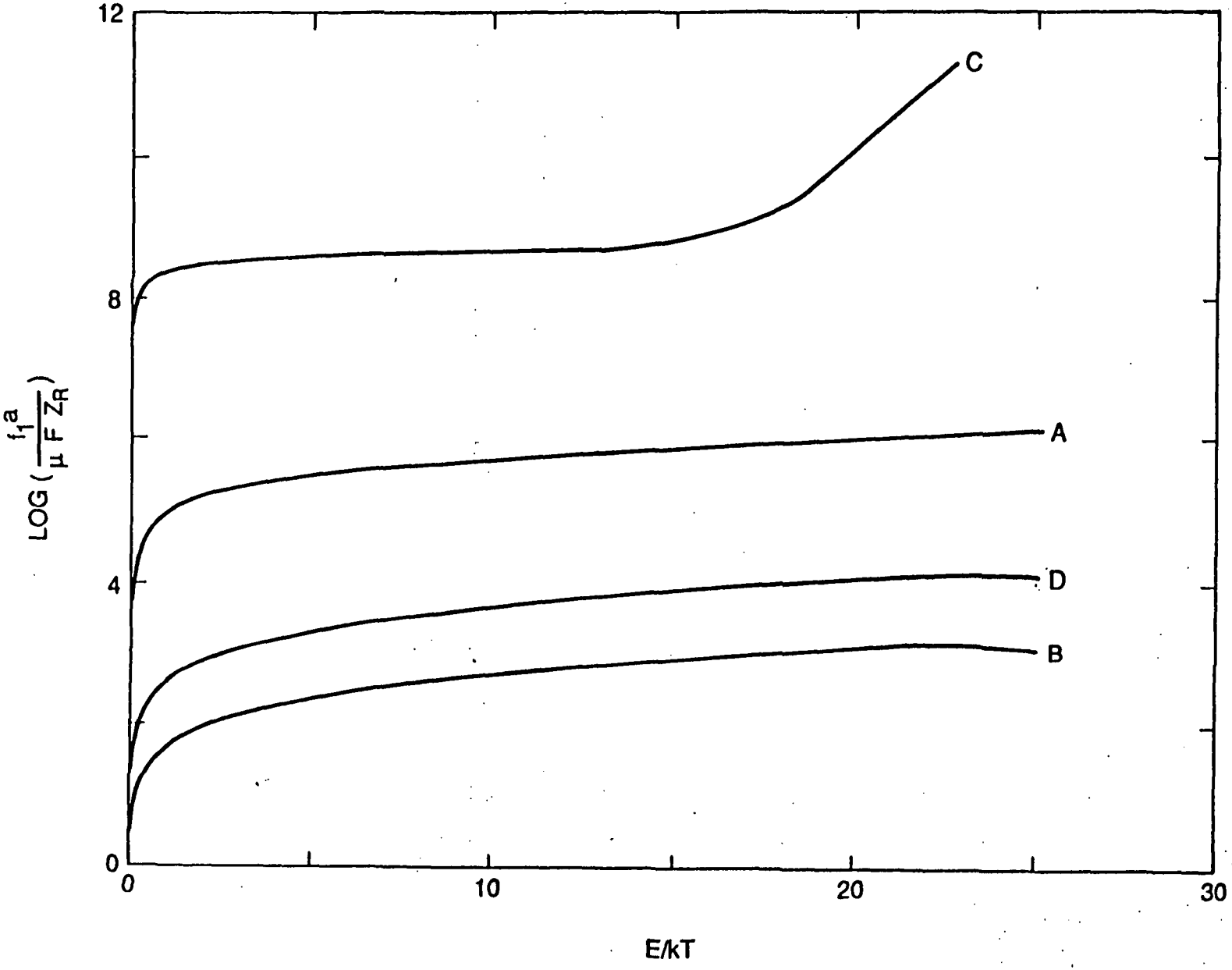

FIG. 8D

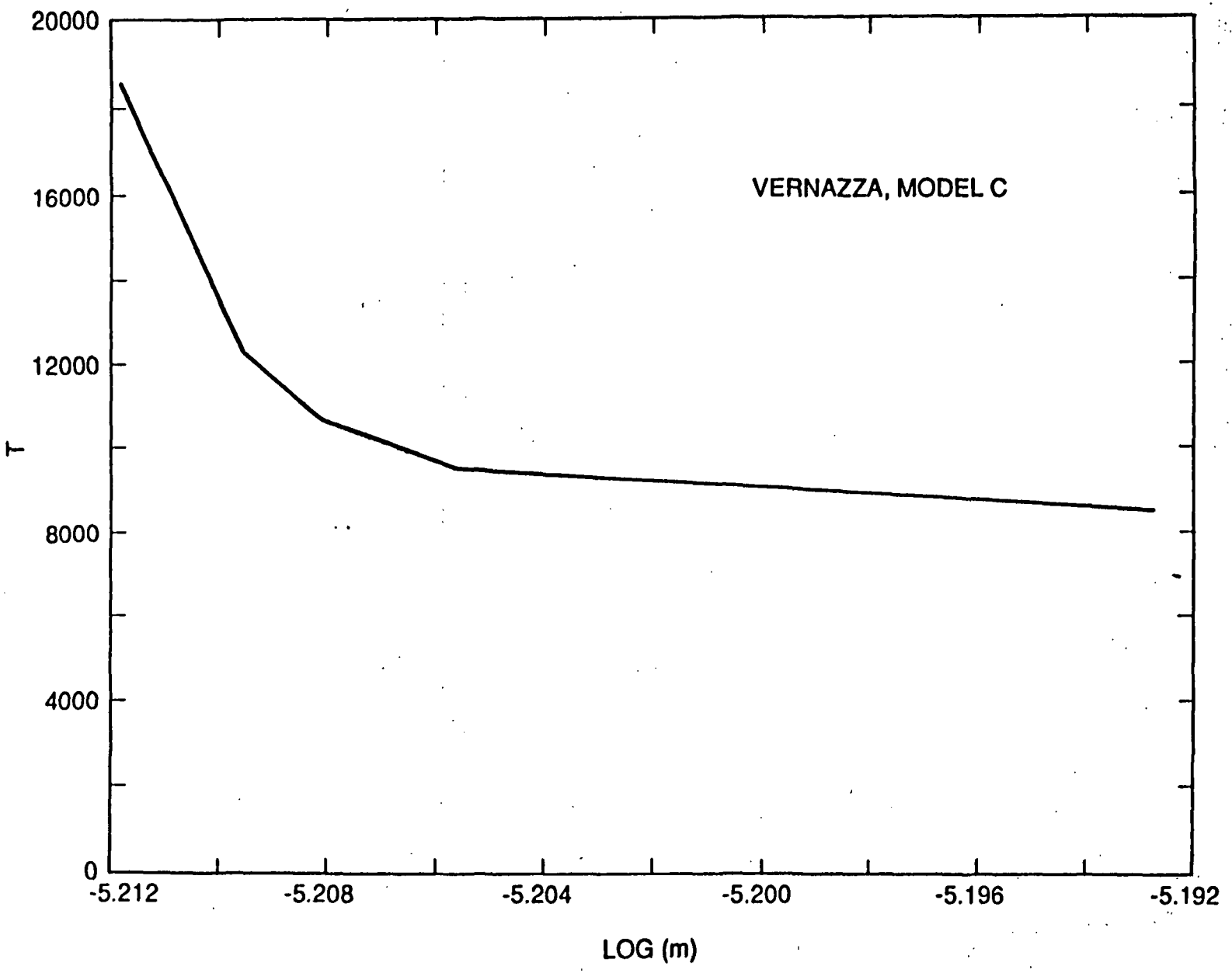
VERNAZZA, MODEL C
T
20000
16000
12000
8000
4000
0
-5.212
-5.208
-5.204
-5.200
-5.196
-5.192
LOG (m)

FIG. 9A

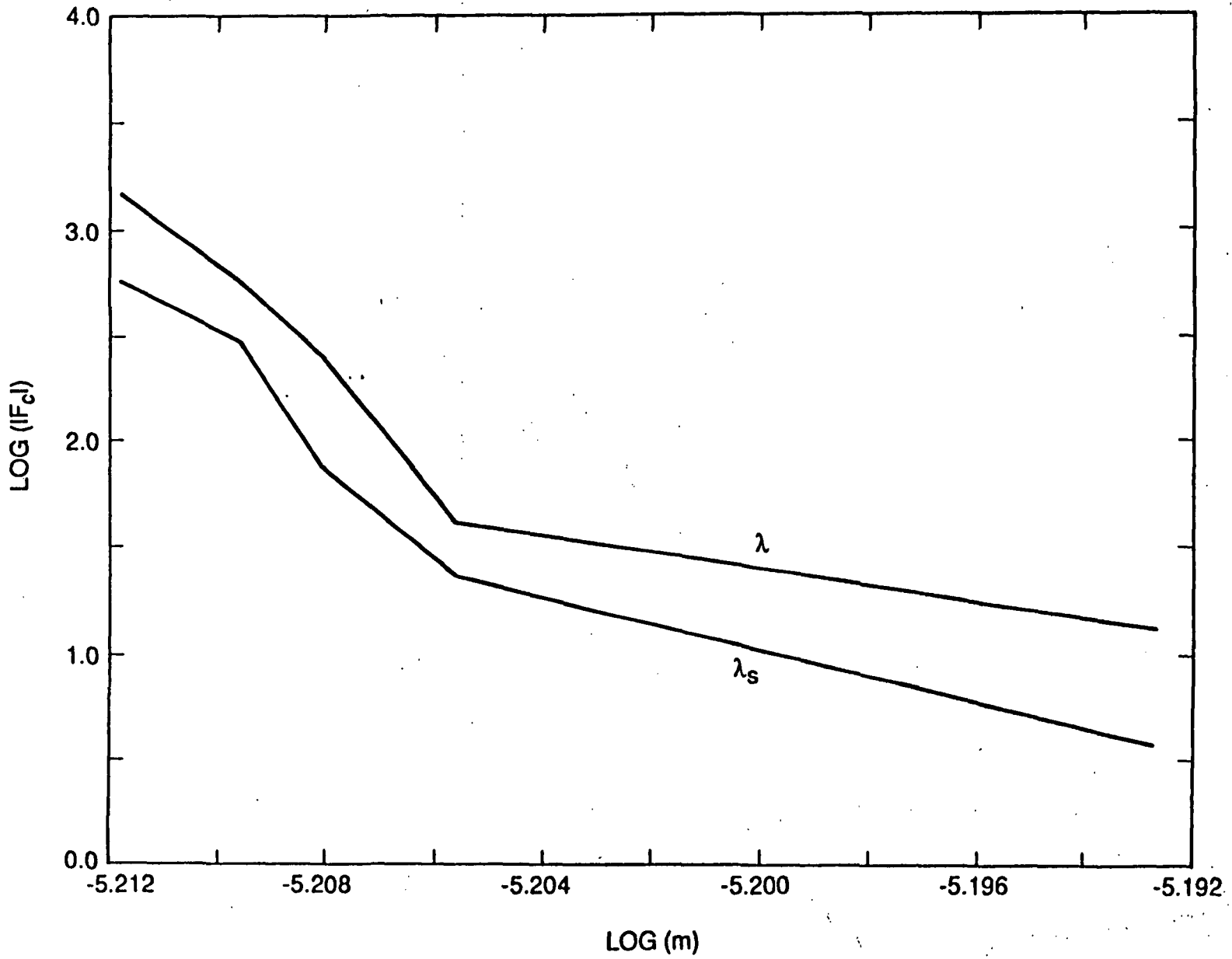

FIG. 9B

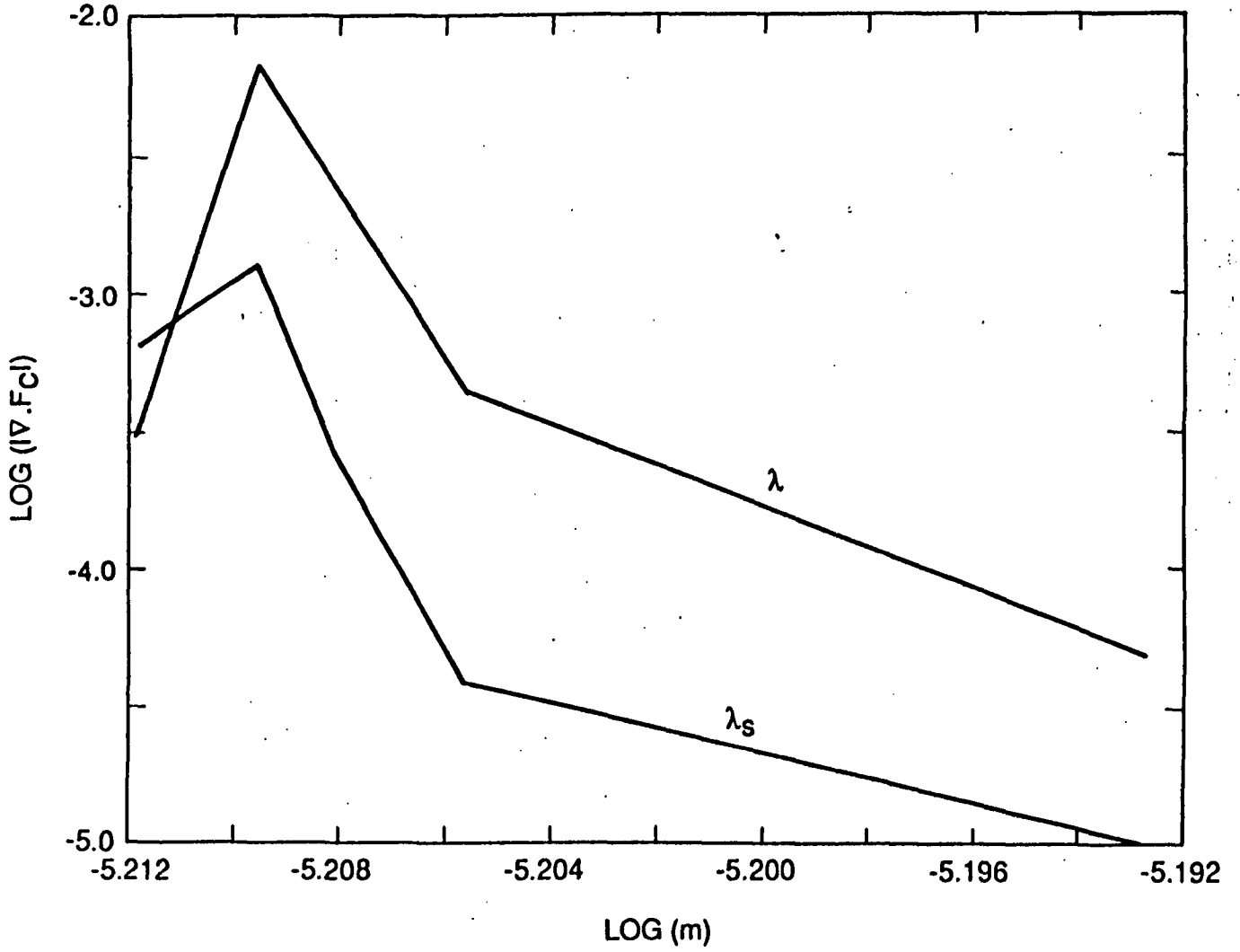

FIG. 9C